



1 SYNERGY BETWEEN SATELLITE OBSERVATIONS OF SOIL MOISTURE 2 AND WATER STORAGE ANOMALIES FOR RUNOFF ESTIMATION

3 Stefania Camici ⁽¹⁾, Gabriele Giuliani ⁽¹⁾, Luca Brocca ⁽¹⁾, Christian Massari ⁽¹⁾, Angelica Tarpanelli
4 ⁽¹⁾, Hassan Hashemi Farahani ⁽²⁾, Nico Sneeuw ⁽²⁾, Marco Restano ⁽³⁾, Jérôme Benveniste ⁽⁴⁾

5 *(1) National Research Council, Research Institute for Geo-Hydrological Protection, Perugia, Italy (s.camici@irpi.cnr.it)*

6 *(2) Institute of Geodesy, University of Stuttgart, Geschwister-Scholl-Straße 24D, 70174 Stuttgart, Germany*

7 *(3) SERCO c/o ESA-ESRIN, Largo Galileo Galilei, Frascati, 00044, Italy*

8 *(4) European Space Agency, ESA-ESRIN, Largo Galileo Galilei, Frascati, 00044, Italy*

9

10

11

12

13

14

15

16

17

18

November 2020

19

Submitted to:

20

* Correspondence to: Ph.D. Stefania Camici, Research Institute for Geo-Hydrological Protection, National Research Council, Via della Madonna Alta 126, 06128 Perugia, Italy. Tel: +39 0755014419 Fax: +39 0755014420 E-mail: stefania.camici@irpi.cnr.it.

21 **ABSTRACT**

22 This paper presents an innovative approach, STREAM - SaTellite based Runoff Evaluation And
23 Mapping - to derive daily river discharge and runoff estimates from satellite soil moisture,
24 precipitation and terrestrial water storage anomalies observations. Within a very simple model
25 structure, the first two variables (precipitation and soil moisture) are used to estimate the quick-flow
26 river discharge component while the terrestrial water storage anomalies are used for obtaining its
27 complementary part, i.e., the slow-flow river discharge component. The two are then summed up to
28 obtain river discharge and runoff estimates.

29 The method is tested over the Mississippi river basin for the period 2003-2016 by using Tropical
30 Rainfall Measuring Mission (TRMM) Multi-satellite Precipitation Analysis (TMPA) precipitation
31 data, European Space Agency Climate Change Initiative (ESA CCI) soil moisture data and Gravity
32 Recovery and Climate Experiment (GRACE) terrestrial water storage data. Despite the model
33 simplicity, relatively high-performance scores are obtained in river discharge simulations, with a
34 Kling-Gupta efficiency index greater than 0.65 both at the outlet and over several inner stations used
35 for model calibration highlighting the high information content of satellite observations on surface
36 processes. Potentially useful for multiple operational and scientific applications (from flood warning
37 systems to the understanding of water cycle), the added-value of the STREAM approach is twofold:
38 1) a simple modelling framework, potentially suitable for global runoff monitoring, at daily time scale
39 when forced with satellite observations only, 2) increased knowledge on the natural processes, human
40 activities and on their interactions on the land.

41

42 Key words: satellite products, soil moisture, water storage variations, conceptual hydrological
43 modelling, rainfall-runoff modelling, Mississippi.

44 1. INTRODUCTION

45 Spatial and temporal continuous river discharge monitoring is paramount for improving the
46 understanding of the hydrological cycle, for planning human activities related to water use as well as
47 to prevent/mitigate the losses due to extreme flood events. To accomplish these tasks, runoff and river
48 discharge data, which represents the aggregated signal of runoff (Fekete et al., 2012), should be
49 available at adequate spatial/temporal resolution, i.e., at basin scale (basin area larger than 10'000
50 km²) and at monthly time step for water resources management and drought monitoring up to grid
51 scale (few km)/(sub-) daily time step for flood prediction. The accurate continuous (in space and
52 time) runoff and river discharge estimation at finer spatial/temporal resolution is still a big challenge
53 for hydrologists.

54 Traditional in situ observations of river discharge, even if generally characterized by high temporal
55 resolution (up to sub-hourly time step), typically offer little information on the spatial distribution of
56 runoff within a watershed. Moreover, river discharge observation networks suffer from many
57 limitations such as low station density and often incomplete temporal coverage, substantial delay in
58 data access and large decline in monitoring capacity (Vörösmarty et al. 2002). Paradoxically, this
59 latter issue is exacerbated in developing nations (Crochemore et al, 2020), where the knowledge of
60 the terrestrial water dynamics deserves greater attention due to huge damages to settlements and
61 especially the loss of human lives that occurs regularly.

62 This precarious situation has led to growing interest in finding alternative solutions, i.e., model-based
63 or observation-based approaches, for runoff and river discharge monitoring. Model-based
64 approaches, based on the mathematical description of the main hydrological processes (e.g., water
65 balance models, WBMs, global hydrological models, GHMs, e.g., Döll et al., 2003 or, increasing in
66 complexity, land surface models, LSM, e.g., Balsamo et al., 2009; Schellekens et al., 2017), are able
67 to provide comprehensive information on a large number of relevant variables of the hydrological
68 cycle including runoff and river discharge at very high temporal and spatial resolution (up to hourly

69 sampling and 0.05° grid scale). However, the values of simulated water balance components rely on
 70 a massive parameterization of the soil, vegetation and land parameters, which is not always realistic,
 71 and are strongly dependent on the GHM/ LSM models used, analysis periods (Wisser et al., 2010)
 72 and climate forcings selected (e.g Haddeland et al., 2012; Gudmundsson et al., 2012a, b; Prudhomme
 73 et al., 2014; Müller Schmied et al., 2016).
 74 Alternatively, the observation-based approaches exploit machine learning techniques and a
 75 considerable amount of data to describe the physics of the system (i.e. hydraulic and/or hydrologic
 76 phenomena, Solomatine and Ostfeld, 2008) with only a limited number of assumptions. Besides being
 77 simpler than model-based approaches, these approaches still present some limitations. ~~At first, as they~~
 78 rely on a considerable amount of data describing the modelled system's physics, the spatial/temporal
 79 extent and the uncertainty of the resulting dataset is determined by the spatial/temporal coverage and
 80 the accuracy of the forcing data (e.g., see E-RUN dataset, Gudmundsson and Seneviratne, 2016;
 81 GRUN dataset, Ghiggi et al., 2019; FLO1K dataset, Barbarossa et al., 2018). Additional limitations
 82 stem from the employed method to estimate runoff. Indeed, random forests such as employed in
 83 Gudmundsson and Seneviratne, 2016, like other machine learning techniques, are powerful tools for
 84 data driven modeling, but they are prone to overfitting, implying that noise in the data can obscure
 85 possible signals (Hastie et al., 2009). Moreover, the influence of land parameters on continental-scale
 86 runoff dynamics is not taken into account as the underlying hypothesis is that the hydrological
 87 response of a basin exclusively depend on present and past atmospheric forcing. It is easy to
 88 understand that this assumption will only be valid in certain circumstances and might lead to
 89 problems, e.g., over complex terrain (Orth and Seneviratne, 2015) or in cases of human river flow
 90 regulation (Ghiggi et al., 2019).
 91 Remote sensing can provide estimates of nearly all the climate variables of the global hydrological
 92 cycle including soil moisture (e.g., Wagner et al., 2007; Seneviratne et al., 2010), precipitation
 93 (Huffman et al., 2014) and total terrestrial water storage (e.g., Houborg et al., 2012; Landerer and
 94 Swenson, 2012; Famiglietti and Rodell, 2013). It has undeniably changed and improved dramatically

95 the ability to monitor the global water cycle and, hence, runoff. By taking advantage of satellite
96 information, some studies tried to develop methodologies able to optimally produce multivariable
97 datasets from the fusion of in situ and satellite-based observations (e.g., Rodell et al., 2015; Zhang et
98 al., 2018; Pellet et al., 2019). Other studies exploited satellite observations of hydrological variables,
99 e.g., precipitation (Hong et al., 2007), soil moisture (Massari et al., 2014), and geodetic variables (e.g.,
100 Sneeuw et al., 2014; Tourian et al., 2018) to monitor single components of the water cycle in an
101 independent way.

102 Although the majority of these studies provide runoff and river discharge data at basin scale and
103 monthly time step, they deserve to be recalled here as important for the purpose of the present study.
104 In particular, Hong et al. (2007) presented a first attempt to obtain an approximate but quasi-global
105 annual streamflow dataset, by incorporating satellite precipitation data in a relatively simple rainfall-
106 runoff simulation approach. Driven by the multiyear (1998-2006) Tropical Rainfall Measuring
107 Mission Multi-satellite Precipitation Analysis, runoff was independently computed for each global
108 land surface grid cell through the Natural Resources Conservation Service (NRCS) runoff curve
109 number (CN) method (NRCS, 1986) and subsequently routed to the watershed outlet to simulate
110 streamflow. The results, compared to the in situ observed discharge data, demonstrated the potential
111 of using satellite precipitation data for diagnosing river discharge values both at global scale and for
112 medium to large river basins. If, on the one hand, the work of Hong et al. (2007) can be considered
113 as a pioneer study, on the other hand it presents a serious drawback within the NRCS-CN method
114 that lacks a realistic definition of the soil moisture conditions of the catchment before flood events.
115 This aspect is not negligible, as it is well established that soil moisture is paramount in the partitioning
116 of precipitation into surface runoff and infiltration inside a catchment (Brocca et al., 2008). In
117 particular, for the same rainfall amount but different values of initial soil moisture conditions,
118 different flooding effects can occur (see e.g. Crow et al., 2005; Brocca et al., 2008; Berthet et al.,
119 2009; Merz and Blochl, 2009; Tramblay et al., 2010). On this line following Brocca et al. (2009),
120 Massari et al. (2016) presented a very first attempt to estimate global streamflow data by using

121 satellite Soil Moisture Active and Passive (SMAP, Entekhabi et al., 2010) and Global Precipitation
122 Measurement (GPM, [Huffman et al., 2019](#)) products. Although the validation was carried out by
123 routing the monthly surface runoff only in a single basin in Central Italy, the obtained results
124 suggested to dedicate additional efforts in this direction.

125 Among the studies that use satellite observations of hydrological variables for runoff estimation, the
126 hydro-geodetic approaches are undoubtedly worth mentioning, see e.g., [Sneeuw et al., 2014](#) for a
127 comprehensive overview or [Lorenz et al. \(2014\)](#) for an analysis of satellite-based water balance
128 misclosures with discharge as closure term. In particular, the satellite mission Gravity Recovery And
129 Climate Experiment (GRACE), which observed the temporal changes in the gravity field, has given
130 a strong impetus to satellite-driven hydrology research ([Tapley et al., 2019](#)). Since temporal gravity
131 field variations over the continents imply water storage change, GRACE was the first remote sensing
132 system to provide observational access to deeper groundwater storage. The relation between GRACE
133 groundwater storage change and runoff was characterized by [Riegger and Tourian \(2014\)](#), which even
134 allowed the quantification of absolute drainable water storage over the Amazon ([Tourian et al., 2018](#)).
135 In essence the storage-runoff relation describes the gravity-driven drainage of a basin and, hence, the
136 slow-flow processes. Due to GRACE's spatial-temporal resolution, runoff and river discharge are
137 generally available for large basins ($>160'000 \text{ km}^2$) and at monthly time step.

138 Based on the above discussion, it is clear that each approach presents strengths and limitations that
139 enable or hamper the runoff and river discharge monitoring at finer spatial and temporal resolutions.
140 In this context, this study presents an attempt to find an alternative method to derive daily river
141 discharge and runoff estimates at $\frac{1}{4}$ degree spatial resolution exploiting satellite observations and the
142 knowledge of the key mechanisms and processes that act in the formation of runoff, i.e., the role of
143 soil moisture in determining the response of a catchment to precipitation. For that, soil moisture,
144 precipitation and terrestrial water storage anomalies (TWSA) observations are used as input into a
145 simple modelling framework named STREAM v1.3 (SaTellite based Runoff Evaluation And
146 Mapping, version 1.3). Unlike classical land surface models, STREAM exploits the knowledge of the

147 system states (i.e., soil moisture and TWSA) to derive river discharge and runoff, and thus it 1) skips
148 the modelling of the evapotranspiration fluxes which are known to be a non-negligible source of
149 uncertainty (Long et al. 2014), 2) limits the uncertainty associated with the over-parameterization of
150 soil and land parameters and 3) implicitly takes into account processes, mainly human-driven (e.g.,
151 irrigation, change in the land use), that might have a large impact on the hydrological cycle and hence
152 on runoff.

153 The detailed description of the STREAM v1.3 model is given in section 4. The collected datasets and
154 the experimental design for the Mississippi River Basin (section 2) are described in sections 3 and 5,
155 respectively. Results, discussion and conclusions are drawn in section 6, 7 and 8, respectively.

156 2. **STUDY AREA**

157 The STREAM **v1.3** model presented here has been tested and validated over the Mississippi River
158 basin. With a drainage area of about 3.3 million km², the Mississippi River basin is the fourth largest
159 watershed in the world, bordered to the West by the crest of the Rocky Mountains and to the East by
160 the crest of the Appalachian Mountains. According to the Köppen climate classification, the climate
161 is subtropical humid over the southern part of the basin, continental humid with hot summer over the
162 central part, continental humid with warm summer over the eastern and northern parts, whereas a
163 semiarid cold climate affects the western part. The average annual air temperature across the
164 watershed ranges from 4°C in the West to 6°C in the East. On average, the watershed receives about
165 900 mm/year of precipitation (77% as rainfall and 23% as snowfall), more concentrated in the eastern
166 and southern portions of the basin with respect to its northern and western part (Vose et al., 2014).

167 The river flow has a clear natural seasonality mainly controlled by spring snowmelt (coming from
168 the Missouri and the Upper Mississippi, the eastern and the upper part of the basin, respectively, Dyer
169 2008) and by heavy precipitation exceeding the soil moisture storage capacity (mostly occurring in
170 the eastern and southern part of the basin, Berghuijs et al., 2016). The basin is also heavily regulated
171 by the presence of large dams (Global Reservoir and Dam Database GRanD, Lehner et al., 2011)

172 most of them located on the Missouri river, over the Great Plains. In particular, the river reach
173 between Garrison and Gavins Point dams is the portion of the Missouri river where the large main-
174 channel dams have the greatest impact on river discharge providing a substantial reduction in the
175 annual peak floods, an increase on low flows and a reduction on the overall variability of intra-annual
176 discharges (Alexander et al., 2012). The annual average of Mississippi river discharge at the
177 Vicksburg outlet section is equal to $17'500 \text{ m}^3/\text{s}$ (see Table 1). Given the variety of climate and
178 topography across the Mississippi River basin, it is a good candidate to test the suitability of the
179 STREAM v1.3 model for river discharge and runoff simulation.

180 3. DATASETS

181 The datasets used in this study include in situ observations, satellite products and model outputs. The
182 first two datasets have been used as input data to the STREAM v1.3 model. Conversely, the model
183 outputs are used as a benchmark to validate the performance of the STREAM v1.3 model.

184 3.1 In situ Observations

185 In situ observations comprise air temperature (T_{air}) and river discharge data (Q).

186 For T_{air} data the Climate Prediction Center (CPC) Global Temperature data developed by the
187 American National Oceanic and Atmospheric Administration (NOAA) using the optimal
188 interpolation of quality-controlled gauge records of the Global Telecommunication System (GTS)
189 network (Fan et al., 2008) have been used. The dataset, downloadable at
190 (<https://psl.noaa.gov/data/gridded/data.cpc.globaltemp.html>) is available on a global regular
191 $0.5^\circ \times 0.5^\circ$ grid, and provides daily maximum (T_{max}) and minimum (T_{min}) air temperature data from
192 1979 to present. The daily average air temperature data have been generated as the mean of T_{max} and
193 T_{min} of each day.

194 Daily Q data over the study basins have been taken from the Global Runoff Data Center (GRDC,
195 https://www.bafg.de/GRDC/EN/Home/homepage_node.html). In particular, 11 gauging stations
196 located along the main river network of the Mississippi River basin have been selected to represent

197 the spatial distribution of runoff over the basin. The location of these gauging stations along with
198 relevant characteristics (e.g., the upstream basin area, the mean annual river discharge and the
199 presence of upstream dams) are summarized in Table 1. ~~As it can be noted, mean annual river~~
200 ~~discharge ranges from 141 to 17'500 m³/s, and 3 out 11 sections~~ are located downstream big dams
201 (Lehner et al., 2011). In particular, Garrison (the fifth-largest earthen dam in the world), Gavins Point
202 and Kanopolis dams ~~located downstream section 1, 2 and 5 respectively~~ (see Figure 3 and Table 1),
203 ~~are three large dams with~~ a maximum storage of $29'383 \times 10^9 \text{ m}^3$, $0.607 \times 10^9 \text{ m}^3$, and $1.058 \times 10^9 \text{ m}^3$
204 respectively.

205 3.2 Satellite Products

206 Satellite products include observations of precipitation (*P*), soil moisture and TWSA.
207 The satellite *P* dataset used in this study is the Multi-satellite Precipitation Analysis 3B42 Version 7
208 (~~TMPA 3B42 V7~~) estimate produced by the National Aeronautics and Space Administration (NASA)
209 as the $0.25^\circ \times 0.25^\circ$ quasi-global (50°N-S) gridded dataset. The TMPA ~~3B42 V7~~ is a gauged-corrected
210 satellite product, with a latency period of two months after the end of the month of record, available
211 at 3h sampling interval from 1998 to present (2020). Major details about the *P* dataset, downloadable
212 from <http://pmm.nasa.gov/data-access/downloads/trmm>, can be found in Huffman et al. (2007).
213 Soil moisture data have been taken from the European Space Agency Climate Change Initiative (ESA
214 CCI) Soil Moisture project (<https://esa-soilmoisture-cci.org/>) that provides a surface soil moisture
215 product (referred to first 2-3 centimeters of soil) continuously updated in term of spatial-temporal
216 coverage, sensors and retrieval algorithms (Dorigo et al., 2017). In this study, the daily combined
217 ESA CCI soil moisture product v4.2 is used, ~~that~~ is available at global scale with a grid spacing of
218 0.25° , for the period 1978-2016.

219 TWSA have been obtained from the Gravity Recovery And Climate Experiment (GRACE) satellite
220 mission. Here we employ the NASA Goddard Space Flight Center (GSFC) global mascon model,
221 i.e., Release v02.4, (Luthcke et al. 2013). It has been produced based on the mass concentration

(mascon) approach. The model provides surface mass densities on a monthly basis. Each monthly solution represents the average of surface mass densities within the month, referenced at the middle of the corresponding month. The model has been developed directly from GRACE level-1b K-Band Ranging (KBR) data. It is computed and delivered as surface mass densities per patch over blocks of approximately $1^{\circ} \times 1^{\circ}$ or about $12'000 \text{ km}^2$. Although the mascon size is smaller than the inherent spatial resolution of GRACE, the model exhibits a relatively high spatial resolution. This is attributed to a statistically optimal Wiener filtering, which uses signal and noise full covariance matrices. This allows the filter to fine tune the smoothing in line with the signal-to-noise ratio in different areas. That is, the less smoothing, the higher signal-to-noise ratio in a particular area and vice versa. This ensures that the filtering is minimal and aggressive smoothing is avoided when unnecessary. Further details of such a filter can be found in Klees et. al (2008). Importantly, the coloured (frequency-dependent) noise characteristic of KBR data was taken in to account when compiling the GRACE model, which has allowed for a reliable computation of the aforementioned noise full covariance matrices. The coloured (frequency-dependent) noise characteristic of KBR data was taken into account when compiling the model, which has allowed for a reliable computation of these noise and signal covariance matrices. They play a crucial role when filtering and allow ~~to achieve~~ a higher spatial resolution compared to commonly applied GRACE filtering methods such as Gaussian smoothing and/or destriping filters. GRACE data are available for the period 01 January 2003 to 15 July 2016.

241 **3.3 Model Outputs**

242 To establish the quality of the STREAM-~~v1.3~~ model in runoff simulation, monthly runoff (**R**) data
243 obtained from the Global Runoff Reconstruction (GRUN_v1, [https://doi.org/10.3929/ethz-b-](https://doi.org/10.3929/ethz-b-000324386)
244 [000324386](https://doi.org/10.3929/ethz-b-000324386)) have been used for comparison. The GRUN dataset (Ghiggi et al., 2019) is a global
245 monthly *R* dataset derived through the use of a machine learning algorithm trained with in situ **Q**
246 observations of relatively small catchments ($<2500 \text{ km}^2$) and gridded precipitation and temperature

247 derived from the Global Soil Wetness Project Phase 3 (GSWP3) dataset (Kim et al., 2017). The
248 dataset covers the period from 1902 to 2014 and it is provided on a $0.5^\circ \times 0.5^\circ$ regular grid.

249 4. METHOD

250 4.1 STREAM Model: Concept

251 The concept behind the STREAM v1.3 model is that river discharge is a combination of hydrological
252 responses operating at diverse time scales (Blöschl et al., 2013; Rakovec et al., 2016). In particular,
253 river discharge can be considered made up of a *slow-flow component*, produced as outflow of the
254 groundwater storage and of a *quick-flow component*, i.e. mainly related to the surface and subsurface
255 runoff components (Hu and Li, 2018).

256 While the high spatial and temporal (i.e., intermittence) variability of precipitation and the highly
257 changing land cover spatial distribution significantly impact the variability of the *quick-flow*
258 *component* (with scales ranging from hours to days and meters to kilometres depending on the basin
259 size), *slow-flow river discharge* reacts to precipitation inputs more slowly (i.e., months) as water
260 infiltrates, is stored, mixed and is eventually released in times spanning from weeks to months.
261 Therefore, the two components can be estimated by relying upon two different approaches that
262 involve different types of observations. Based on that, within the STREAM v1.3 model, satellite soil
263 moisture, precipitation and TWSA will be used for deriving river discharge and runoff estimates. The
264 first two variables are used as proxy of the *quick-flow* river discharge component while TWSA is
265 exploited for obtaining its complementary part, i.e., the *slow-flow river discharge* component. Firstly,
266 we exploit the role of the soil moisture in determining the response of the catchment to the
267 precipitation inputs, which have been soundly demonstrated in more than ten years of literature
268 studies (see e.g., Brocca et al., 2017 for a comprehensive discussion on the topic). Secondly, we
269 consider the important role of terrestrial water storage in determining the slow-flow river discharge
270 component as modelled in several hydrological models (e.g., Sneeuw et al., 2014).

271 It is worth noting that ~~this *modus operandi*, i.e. to model the quick-flow and slow-flow discharge~~
272 ~~component separately exploring their process controls~~, independently, has been largely applied and
273 tested in recent and past studies, e.g., for the estimation of the flow duration curve (see e.g. Botter et
274 al., 2007a, b; Yokoo and Sivapalan 2011; Muneeppeerakul et al., 2010; Ghotbi et al., 2020).

275 **4.2 STREAM Model: the Laws**

276 The STREAM v1.3 model is a conceptual hydrological model ~~that, by using as input observation of~~
277 ~~P , soil moisture, TWSA and T_{air} data, simulates continuous R and Q time series.~~

278 The model entails three main components (Figure 1): 1) a snow module to separate precipitation into
279 snowfall and rainfall, 2) a soil module to simulate the evolution in time t of the ~~quick and slow~~ runoff
280 responses, Q_{fu} [mm] and Q_{sl} [mm], and 3) a routing module that transfers these components through
281 the basins and the rivers for the simulation of the *quick-flow* river discharge, QF [m³/s], and the *slow-*
282 *flow* river discharge, SF [m³/s] components. The soil module is composed of two storages, Su and Sl
283 as illustrated in Figure 1. The upper storage receives inputs from P , released through a snow module
284 (Cislaghi et al., 2020) as rainfall (~~r~~) or stored as snow water equivalent (SWE) within the snowpack
285 and on the glaciers. In particular, according to Cislaghi et al. (2020), SWE is modelled by using as
286 input T_{air} and a degree-day coefficient, C_m , to be estimated by calibration. We have to acknowledge
287 that, even though this rain/snow differentiation method works quite efficiently at a large grid size like
288 the one used in the study (25 x 25 km), the topographic complexity of higher elevations can be lost.
289 A different differentiation scheme based e.g., on the wet bulb temperature like in IMERG (Wang et
290 al., 2019; Arabzadeh and Behrangi, 2021), would be ~~preferable but is out of the purpose study.~~

291 Once separated, ~~r~~ input contributes to the **quick runoff** response while the SWE (like other fluxes
292 contributing to modify the soil water content into Su) is neglected as already considered in the satellite
293 TWSA. Therefore, the first key point of the STREAM v1.3 model is that the water content in the
294 upper storage is directly provided by the satellite soil moisture observations and the loss processes
295 like infiltration or evaporation do not need to be explicitly modelled to simulate the evolution in time

296 t of soil moisture. Consequently, the quick runoff response, Qfu from the first storage can be
 297 computed following the formulation proposed by Georgakakos and Baumer (1996), as in equation
 298 (1):

$$299 \quad Qfu(t) = r(t) SWI(t, T)^\alpha \quad (1)$$

300 where:

301 - SWI is the Soil Water Index (Wagner et al., 1999), i.e., the root-zone soil moisture product referred
 302 to the first layer of the model (representative of the first 5-30 centimeters of soil), derived by the
 303 surface satellite soil moisture product, θ , by applying the exponential filtering approach in its
 304 recursive formulation (Albergel et al., 2009):

$$305 \quad SWI_n = SWI_{n-1} + K_n(\theta(t_n) - SWI_{n-1}) \quad (2)$$

306 with the gain K_n at the time t_n given by:

$$307 \quad K_n = \frac{K_{n-1}}{K_{n-1} + e^{\left(\frac{t_n - t_{n-1}}{T}\right)}} \quad (3)$$

- 308 - T [days] is a parameter, named characteristic time length, that characterizes the temporal variation
- 309 of soil moisture within the root-zone profile and the gain K_n ranges between 0 and 1;
- 310 - $\alpha[-]$ is a coefficient linked to the non-linearity of the infiltration process and it takes into account
- 311 the characteristics of the soil;
- 312 - for the initialization of the filter $K_1 = 1$ and $SWI_1 = \theta(t_1)$.

313 The second key point of STREAM v1.3 model concerns the estimation of the slow runoff response,
 314 Qsl , from the second storage. The hypothesis here, shared also with other studies (e.g., Rakovec et al.,
 315 2016), is that the dynamic of the slow runoff component can be represented by the monthly TWSA
 316 data. Indeed, the time scale of slow runoff response is typically in the range of seasons to years and it
 317 can be assumed almost independent upon the water that is contained in that upper storage. For that, the

slow runoff response Q_{sl} , from the second storage, can be computed following the formulation proposed by Famiglietti and Wood (1994), through equation (4) as follows:

$$Q_{sl}(t) = \beta (TWSA^*(t))^m \quad (4)$$

where:

- $TWSA^*$ [-] is the TWSA estimated by GRACE normalized by its minimum and maximum values. The assumption behind this equation is that TWSA can be assumed as a proxy of the evolution in time, t , of the Sl , i.e., the ~~storage of the~~ lower storage.
- β [mm h⁻¹] and m [-] are two parameters describing the nonlinearity between slow runoff component and $TWSA^*$.

Note that we made the hypothesis that soil moisture and TWSA observations are independent (whereas in the reality soil moisture can be responsible both for the generation of the quick flow part (mainly) and for the slow flow contribution) given the different temporal (and spatial) scales at which the quick and slow runoff responses act.

The STREAM v1.3 model runs in a semi-distributed version in which the catchment is divided into s elements, each one representing either a subcatchment with outlet along the main channel or an area draining directly into the main channel. Each element is assumed homogeneous and hence constitutes a lumped system.

The routing module (~~controlled by a γ parameter~~) conveys the Q_{fu} and Q_{sl} response components at each element outlet (subcatchments and directly draining areas, Brocca et al., 2011) and successively at the catchment outlet of the basin. Specifically, the quick component Q_{fu} is routed to the element outlet by the Geomorphological Instantaneous Unit Hydro-graph (GIUH, Gupta et al., 1980) for subcatchments or through a linear reservoir approach (Nash, 1957) for directly draining areas; the Q_{sl} slow component is transferred to the outlet section by a linear reservoir approach. Finally, a diffusive linear approach (controlled by the parameters C and D , i.e., Celerity and Diffusivity,

342 Troutman and Karlinger, 1985) is applied to route the quick and slow runoff components at the outlet
343 section of the catchment (Brocca et al., 2011). In the first case we obtain the *quick-flow* river discharge
344 component, QF [m^3/s], and in the second case the *slow-flow* river discharge component, SF [m^3/s]
345 (see Figure 1).

346 **4.3 STREAM Parameters**

347 The STREAM v1.3 model uses 8 parameters of which 5 are used in the soil module (α , T [days], β
348 [$mm\ h^{-1}$], m , C_m) and 3 in the routing module (γ , C [$km\ h^{-1}$] and D [$km^2\ h^{-1}$]). The parameter values,
349 determined within the feasible parameter space (See Table Appendix A for more details), are
350 calibrated by maximizing the Kling-Gupta Efficiency index (KGE, Gupta et al., 2009; Kling et al.,
351 2012, see paragraph 5.1 for more details) between observed and simulated river discharge. For model
352 calibration, a standard gradient-based automatic optimisation method (Bober 2013) was used.

353 **5. EXPERIMENTAL DESIGN**

354 **5.1 Modelling Setup for Mississippi River Basin**

355 The modelling setup is carried out in three steps (Figure 2):

356 1. *Sub-basin delineation*. STREAM v1.3 model is run in the semi-distributed version over the
357 Mississippi River basin. The TopoToolbox (<https://topotoolbox.wordpress.com/>), a tool developed in
358 Matlab by Schwanghart et al. (2010), and the SHuttle Elevation Derivatives at multiple Scales
359 (HydroSHED, <https://www.hydrosheds.org/>) DEM of the basin at the 3'' resolution (nearly 90 m at
360 the equator) have been used to derive flow directions, to extract the stream network and to delineate
361 the drainage basins over the Mississippi River basin. In particular, by considering only rivers with
362 order greater than 3 (according to the Horton-Strahler rules, Horton, 1945; Strahler, 1952), the
363 Mississippi watershed has been divided into 53 sub-basins as illustrated in Figure 3. Red dots in the
364 figure indicate the location of the 11 discharge gauging stations selected for the study area.

~~It has to be specified that the step of sub-basin delineation could be accomplished through tools different from the TopoToolbox. For instance, it could be used the free Qgis software downloadable at <https://www.qgis.org/it/site/forusers/download.html>, following the instruction to perform the hydrological analysis as in https://docs.qgis.org/3.16/en/docs/training_manual/processing/hydro.html?highlight=hydrological%20analysis.~~

2. *Extraction of input data.* Precipitation, T_{air} , soil moisture and TWSA datasets data have to be extracted for each sub-basin of the study area. If characterized by different spatial/temporal resolution, these datasets need to be resampled over a common spatial grid/temporal time step prior to be used as input into the model.

To run the STREAM v1.3 model over the Mississippi river basin, input data have been resampled over the precipitation spatial grid at 0.25° resolution through a bilinear interpolation. Concerning the temporal scale, T_{air} , soil moisture and precipitation data are available at daily time step, while monthly TWSA data have been linearly interpolated at daily time step. For each of the 53 Mississippi subbasins, the resampled precipitation, soil moisture, T_{air} and TWSA data have been extracted.

3. *STREAM model calibration.* In situ river discharge data are used as reference data for the calibration of STREAM v1.3 model. For Mississippi, the STREAM v1.3 model has been calibrated over five sections as illustrated in Figure 3: the inner sections 4, 6, 9, 11 and the outlet section 10, are used to calibrate the model and all sub-basins contributing to the respective sections are highlighted with the same colour. This means that, for example, the sub-basins labelled as 1, 2, 5 to 15, 17, 22, 23, and 30 contribute to section 4, sub-basins 31, 37, 38 and 41 contribute to section 6 and so on. Consequently, the sub-basins highlighted with the same colour are assigned the same model parameters, i.e. the parameters that allow to reproduce the river discharge data observed at the related outlet section.

Once calibrated, the STREAM v1.3 model has been run to provide continuous daily **Q and R** time series, at the outlet section of each subbasin and over each grid pixel, respectively. By considering

391 the spatial/temporal availability of both in situ and satellite observations, the entire analysis period
392 covers the maximum common observation period, i.e., from 01 January 2003 to 15 July 2016 at daily
393 time scale. To establish the goodness-of-fit of the model, the simulated river discharge and runoff
394 timeseries are compared against in situ river discharge and modelled runoff data.

395 **5.2 Model Evaluation Criteria and Performance Metrics**

396 The model has been run over a 13.5-year period split into two sub periods: the first 8 years, from
397 January 2003 to December 2010, have been used to calibrate the model, ~~successively validated over~~
398 ~~the remaining 5.5 years~~ (January 2011 - July 2016).

399 In particular, three different validation schemes have been adopted to assess the robustness of the
400 STREAM v1.3 model:

- 401 1. Internal validation aimed to test the plausibility of both the model structure and the parameter
402 set in providing reliable estimates of the hydrological variables against which the model is
403 calibrated. For this purpose, a comparison between observed and simulated river discharge
404 time series on the sections used for model calibration has been carried out for both the
405 calibration and validation sub periods.
- 406 2. Cross-validation testing the goodness of the model structure and the calibrated model
407 parameters to predict hydrological variables at locations not considered in the calibration
408 phase. In this respect, the cross-validation has been carried out by comparing observed and
409 simulated river discharge time series in gauged basins not considered during the calibration
410 phase;
- 411 3. External validation aimed to test the capability of the model “*to get the right answers for the*
412 *right reasons*” (Kirchner 2006). The rationale behind this concept is that the hydrological
413 models are today highly performing and able to reproduce a lot of hydrological variables. For
414 that, the model performances should not only be evaluated against observed streamflow, but
415 complementary datasets representing internal hydrologic states and fluxes (e.g., soil moisture,
416 evapotranspiration, runoff etc) should be considered. As runoff is a secondary product of the

STREAM v1.3 model, obtained indirectly from the calibration of the river discharge (basin-integrated runoff), the comparison in terms of runoff can be considered as a further external validation of the model. Runoff, differently from discharge, cannot be directly measured. It is generally modelled through land surface or hydrological models. Its validation requires a comparison against modelled data that, however, suffer from uncertainties (Beck et al., 2017). Based on that, in this study the GRUN runoff dataset described in the section 3.3 has been used for a qualitative comparison.

5.3 Performance Metrics

To measure the goodness-of-fit between simulated and observed river discharge data three performance scores have been used:

- the relative root mean square error, RRMSE:

$$RRMSE = \frac{\sqrt{\frac{1}{n} \sum_{i=1}^n (Q_{sim_i} - Q_{obs_i})^2}}{\frac{1}{n} \sum_{i=1}^n (Q_{obs_i})} \quad (5)$$

where Q_{obs} and Q_{sim} are the observed and simulated discharge time series of length n . RRMSE values range from 0 to $+\infty$, the lower the RRMSE, the better the agreement between observed and simulated data.

- the Pearson correlation coefficient, R , measures the linear relationship between two variables:

$$R = \frac{\sum_{i=1}^n (Q_{sim_i} - \overline{Q_{sim}})(Q_{obs_i} - \overline{Q_{obs}})}{\sqrt{\sum_{i=1}^n (Q_{sim_i} - \overline{Q_{sim}})^2 (Q_{obs_i} - \overline{Q_{obs}})^2}} \quad (6)$$

where $\overline{Q_{obs}}$ and $\overline{Q_{sim}}$ represent the mean values of Q_{obs} and Q_{sim} , respectively. The values of R range between -1 and 1 ; higher values of R indicate a better agreement between observed and simulated data.

- the Kling-Gupta efficiency index (KGE, Gupta et al., 2009), which provides direct assessment of four aspects of discharge time series, namely shape, timing, water balance and variability. It is defined as follows:

$$KGE = 1 - \sqrt{(R - 1)^2 + (\delta - 1)^2 + (\varepsilon - 1)^2} \quad (7)$$

441 where R is the correlation coefficient, δ the relative variability and ε the bias normalized by the
442 standard deviation between observed and simulated discharge. The KGE values range between $-\infty$
443 and 1; the higher the KGE, the better the agreement between observed and simulated data.
444 Simulations characterized by values of KGE in the range -0.41 and 1 can be assumed as reliable;
445 values of KGE greater than 0.5 have been assumed good with respect to their ability to reproduce
446 observed time series (Thiemig et al., 2013).

447 **6. RESULTS**

448 The testing and validation of the STREAM v1.3 model is presented and discussed in this section
449 according to the scheme illustrated in section 5.2.

450 **6.1 Internal Validation**

451 The performance of the STREAM v1.3 model over the calibrated river sections is illustrated in Figure
452 4 and summarized in Table 2. Figure 4 shows observed and simulated river discharge time series over
453 the whole study period (2003-2016); in Table 2 the performance scores are evaluated separately for
454 the calibration and validation sub periods. It is worth noting that the model accurately simulates the
455 observed river discharge data and is able to give the “right answer” with good modelling
456 performances. Score values of KGE and R over the calibration (validation) period are higher than
457 0.62 (0.67) and 0.75 (0.75) (resp.) for all the sections; RRMSE is lower than 46% (51%) for all the
458 sections except for section 9, where it rises up to 71% (77%). The performances remain good even if
459 they are evaluated over the entire study period as indicated by the scores on the top of each plot of
460 Figure 4.

461 **6.2 Cross-validation**

462 The cross-validation has been carried out over the six river sections illustrated in Figure 5 not used
463 in the calibration step. The performance scores on the top of each plot refer to the entire study periods;
464 the scores split for calibration and validation periods are reported in Table 2. For some river sections
465 the performance is quite low (see, e.g., river section 1, 2 and 5) whereas for others the model is able

to simulate the observed discharge data quite accurately (e.g., 7 and 8). In particular, for river sections 1 and 2 even if KGE reaches values equal to 0.35 and 0.40 (for the whole period), respectively, there is not a good agreement between observed and simulated river discharge and the R score is lower than 0.55 for both river sections. The worst performance is obtained over section 5, with negative KGE and low R (high RRSME). These results are certainly influenced by the presence of large dams located upstream to these river sections (i.e., Garrison, Gavins Point and Kanopolis dams, see Table 1) which have a strong impact on discharge: the model, not having a specific module for modelling reservoirs, is not able to accurately reproduce the dynamics of river discharge over regulated river sections. Positive KGE values are obtained over river sections 3, 7 and 8. In particular, over section 3 the STREAM v1.3 model overestimates the observed river discharge due the presence of large dams along the Missouri river, over the Great Plains region. This area is well known from other large-scale hydrological models (e. g., ParFlow-CLM and WRF-Hydro) to be an area with very low performances in terms of river discharge modelling (O'Neill et al., 2020, Tijerina et al., 2021).

Over section 7, located over the Rock river, a relatively small tributary of Mississippi river (see Table 1), the STREAM v1.3 model overestimation has to be attributed to: 1) the different characteristics of the Rock river basin with respect to the entire basin closed to section 6 where the model has been calibrated (see Figure 3); 2) the small size of the Rock river basin ($23'000 \text{ km}^2$, if compared with GRACE resolution, $160'000 \text{ km}^2$) for which the model accuracy is expect to be lower. Conversely, the performances over river section 8, whose parameters have been set equal to the ones of river section 10, are quite high (KGE equal to 0.71, 0.80 and 0.77 for the entire, the calibration and the validation period, respectively; R equal to 0.83, 0.84 and 0.84 for the entire, calibration and validation periods, respectively). This outcome demonstrates that under some circumstances, the STREAM v1.3 model can be used to estimate river discharge in basins not calibrated over, especially those without upstream dams and with comparable size and land cover.

Although it is expected that the performances of STREAM v1.3 model, as any hydrological model calibrated against observed data, can decrease over the gauging sections not used for the calibration,

the findings obtained above raises doubts about the robustness of model parameters and whether it is actually possible to transfer model parameters from one river section to another with different interbasin characteristics. A more in-depth investigation about the model calibration procedure, with special focus on the regionalization of the model parameters, should be carried out but this topic is beyond the scope of the manuscript.

6.3 External Validation

For the external validation, the monthly runoff time series provided by the GRUN datasets have been compared against the ones computed by the STREAM v1.3 model. For that, STREAM daily runoff time series have been aggregated at monthly scale and re-gridded at the same spatial resolution of the GRUN dataset (0.5°). The comparison is illustrated in Figure 6 for the common period 2003–2014. Although the two datasets consider different precipitation inputs, the two models agree in identifying two distinct zones in terms of runoff, i.e., the western dry and the eastern wet area. This two distinct zones can be clearly identified also in the GSWP3 and TMPA 3B42 V7 precipitation maps (see Figure S1) used as input in GRUN and STREAM v1.3, respectively, stressing that STREAM runoff output is correctly driven by the input data. However, likely due to the calibration procedure, the STREAM runoff map appears patchier with respect to GRUN and discontinuities along the sub-basin boundaries (identified in Figure 3) can be noted. This should be ascribed to the automatic calibration procedure of the model that, differently from other calibration techniques (e. g., regionalization procedures), does not consider the basin physical attributes like soil, vegetation, and geological properties that govern spatial dynamics of hydrological processes. This calibration procedure can generate sharp discontinuities even for neighbouring subcatchments individually calibrated. It leads to discontinuities in model parameter values and consequently in the simulated hydrological variable (runoff).

515 7. DISCUSSION

516 In the previous sections, the ability of the STREAM v1.3 model to accurately simulate river discharge
517 and runoff time series has been presented. In particular, Figures 4, 5 and 6 demonstrate that satellite
518 observations of precipitation, soil moisture and terrestrial water storage anomalies can provide
519 accurate daily river discharge estimates for near-natural large basins (absence of upstream dams), and
520 for basins with draining area lower than 160'000 km² (see section 7), i.e., at spatial/temporal
521 resolution lower than the ones of the TWSA input data (monthly, 160'000 km²). This is an important
522 result of the study as it demonstrates, on one hand, that the model structure is appropriate with respect
523 to the data used as input and, on the other hand, the great value of information contained into TWSA
524 data that, even if characterized by limited spatial/temporal resolution, can be used to simulate runoff
525 and river discharge at basin scale. This finding has been also confirmed by a preliminary sensitivity
526 analysis in which the STREAM v1.3 model has been run with different hydrological inputs of
527 precipitation, soil moisture and total water storage anomaly (not shown here for brevity). In particular,
528 by running the STREAM v1.3 model with different input configurations (e.g., by using TMPA 3B42
529 V7 or Climate Prediction Center (CPC) data for precipitation, ESA CCI or Advanced SCATterometer
530 (ASCAT) data for soil moisture, TWSA or soil moisture data to simulate the slow-flow river
531 discharge component), we found that STREAM results are more sensitive to soil moisture data rather
532 than to precipitation input. In addition, by running STREAM v1.3 model with soil moisture data as
533 input to simulate the slow-flow river discharge component (i.e. without using TWSA data) we found
534 a deterioration of the model results.

535 Hereinafter, the strengths and the main limitations of the STREAM v1.3 model are discussed.

536 Among the strengths of the STREAM v1.3 model it is worth highlighting:

537 1. **Simplicity.** The STREAM v1.3 model structure: 1) limits the input data required (only
538 precipitation, air temperature, soil moisture and TWSA data are needed as input; LSM/GHMs require
539 many additional inputs such as wind speed, shortwave and longwave radiation, pressure and relative

540 humidity); 2) limits and simplifies the processes to be modelled for runoff/discharge simulation.
541 Processes like evapotranspiration, infiltration or percolation, are not modelled therefore avoiding the
542 need of using sophisticated and highly parameterized equations (e.g., Penman-Monteith for
543 evapotranspiration, Allen et al.,1998, Richard equation for infiltration, Richard, 1931); 3) limits the
544 number of parameters (only 8 parameters have to be calibrated) thus simplifying the calibration
545 procedure and potentially reduce the model uncertainties related to the estimation of parameter
546 values.

547 **2. Versatility.** The STREAM v1.3 model is a versatile model suitable for daily runoff and discharge
548 estimation over sub-basins with different physiographic characteristics. The results obtained in this
549 study clearly indicate the potential of this approach to be extended at the global scale. Moreover, the
550 model can be easily adapted to ingest input data with spatial/temporal resolution different from the
551 one tested in this study (0.25°/daily). For instance, satellite missions with higher space/time
552 resolution, or near real time satellite products could be considered. As an example, the Next
553 Generation Gravity Mission design studies all encompass double-pair scenarios, which would greatly
554 improve upon the current spatial resolution of single-pair missions like GRACE and GRACE-FO (>
555 100'000 km²). The STREAM v1.3 model shows high flexibility also in the possibility to modify the
556 subbasin delineation and to introduce additional observational river discharge data to be used for the
557 model calibration.

558 **3. Computationally inexpensive.** Due to its simplicity and the limited number of parameters to be
559 calibrated, the computational effort for the STREAM v1.3 model is very limited.”

560 However, some limitations have to be acknowledged for the current version of the STREAM v1.3
561 model:

562 **1. Presence of reservoir, diversion, dams or flood plain.** As the STREAM v1.3 model does not
563 explicitly consider the presence of discontinuity elements along the river network (e. g, reservoir,
564 dam or floodplain), discharge estimates obtained for sections located downstream of such elements
565 might be inaccurate (see, e.g., river sections 1 and 2 in Figure 5).

566 **2. Need of in situ data for model calibration and robustness of model parameters.** As discussed
567 in the results section, parameter values of the STREAM v1.3 model are set through an automatic
568 calibration procedure aimed at minimizing the differences between simulated and observed river
569 discharge. The main drawback of this parameterization technique ~~is that the models parameterized~~
570 ~~with this technique may exhibit~~ (1) poor predictability of state variables and fluxes at locations and
571 periods not considered in the calibration, and (2) sharp discontinuities along sub-basin boundaries in
572 state flux, and parameter fields (e.g., Merz and Blöschl, 2004). To overcome these issues, several
573 regionalization procedures, as for instance summarized in Cislaghi et al. (2020), could be
574 conveniently applied to transfer model parameters from hydrologically similar catchments to a
575 catchment of interest. In particular, the regionalization of model parameters could allow to: i) estimate
576 discharge and runoff time series over ungauged basins overcoming the need of discharge data
577 recorded from in-situ networks; ii) estimate the model parameter values through a physically
578 consistent approach, linking them to the characteristics of the basins; iii) solve the problem of
579 discontinuities in the model parameters, avoiding to obtain patchy unrealistic runoff maps. As this
580 aspect requires additional investigations and it is beyond the paper purpose, it will not be tackled
581 here.

582 By looking at technical reviews of large-scale hydrological models (e.g., Sood and Smakhtin, 2015,
583 Kauffeldt et al., 2016), it can be noted there are many established models, similar in objective and
584 limitations to STREAM v1.3 model, already existing with support and user base (e.g., among others,
585 Community Land Model, CLM, Oleson et al., 2013; European Hydrological Predictions for the
586 Environment, E-HYPE, Lindström et al., 2010; H08, Hanasaki et al., 2008, PCR-GLOBWB, van
587 Beek and Bierkens, 2008; Water – a Global Assessment and Prognosis WaterGAP, Alcamo et al.,
588 2003; ParFlow-CLM, Maxwell et al., 2015; WRF-Hydro, Gochis et al., 2018). Some of them, e.g.,
589 ParFlow-CLM or WRF-Hydro have been specifically configured across the continental United States
590 and showed good capability to reproduce observed streamflow data over the Mississippi river basin

591 with performances decreased throughout the Great Plains (O'Neill et al., 2020, Tijerina et al., 2021)
592 which is consistent with the results we obtained with STREAM v1.3 model. However, with respect
593 to classical hydrological and land surface models, STREAM v1.3 is based on a new concept for
594 estimating runoff and river discharge which relies on: (a) the almost exclusive use of satellite
595 observations, and, (b) a simplification of the processes being modelled.
596 This approach brings several advantages: 1) satellite data implicitly consider the human impact on
597 the water cycle observing some processes, such as irrigation application or groundwater withdrawals,
598 that are affected by large uncertainty in classical hydrological models, 2) the satellite technology
599 grows quickly and hence it is expected that the spatial/temporal resolution and accuracy of satellite
600 products will be improved in the near future (e.g., 1 km resolution from new satellite soil moisture
601 products and the next generation gravity mission); the STREAM v1.3 model is able to fully exploit
602 such improvements; 3) STREAM v1.3 model simulates only the most important processes affecting
603 the generation of runoff, and considers only the most important variables as input (precipitation,
604 surface soil moisture and groundwater storage). In other words, the model does not need to simulate
605 processes, such as evapotranspiration and infiltration and therefore it is an independent modelling
606 approach for simulating runoff and river discharge that can be also exploited for benchmarking and
607 improving classical land surface and hydrological models.

608 **8. CONCLUSIONS**

609 This study presents a new conceptual hydrological model, STREAM v1.3, for runoff and river
610 discharge estimation. By using as input satellite data of precipitation, soil moisture and terrestrial
611 water storage anomalies, the model has been able to provide accurate daily river discharge and runoff
612 estimates at the outlet river section and the inner river sections and over a $0.25^{\circ} \times 0.25^{\circ}$ spatial grid of
613 the Mississippi river basin. In particular, the model is suitable to reproduce:
614 1. river discharge time series over the calibrated river section with good performances both in
615 calibration and validation periods;

616 2. river discharge time series over river sections not used for calibration and not located downstream
617 dams or reservoirs;

618 3. runoff time series with a quite good agreement with respect to the well-established GRUN
619 observational-based dataset used for comparison.

620 The integration of observations of soil moisture, precipitation and terrestrial water storage anomalies
621 is a first alternative method for river discharge and runoff estimation with respect to classical methods
622 based on the use of TWSA-only (suitable for river basins larger than 160'000 km², monthly time
623 scale) or on classical LSMs (Cai et al., 2014).

624 Moreover, although simple, the model has demonstrated a great potential to be easily applied over
625 subbasins with different climatic and topographic characteristics, suggesting also the possibility to
626 extend its application to other basins. In particular, the analysis over basins with high human impact,
627 where the knowledge of the hydrological cycle and the river discharge monitoring is very important,
628 deserves special attention. Indeed, as the STREAM v1.3 model is directly ingesting observations of
629 soil moisture and terrestrial water storage data, it allows the modeller to neglect processes that are
630 implicitly accounted for in the input data. Therefore, human-driven processes (e.g., irrigation, land
631 use change), that are typically very difficult to simulate due to missing information and might have a
632 large impact on the hydrological cycle, hence on total runoff, could be implicitly modelled. The
633 application of the STREAM v1.3 model on a larger number of basins with different climatic-
634 physiographic characteristics (e.g., including more arid basins, snow-dominated, lots of topography,
635 heavily managed) will allow to investigate the possibility to regionalize the model parameters and
636 overcome the limitations of the automatic calibration procedure highlighted in the discussion section.

637 **AUTHOR CONTRIBUTION**

638 S.C. performed the analysis and wrote the manuscript. G.G. collected the data and helped in
639 performing the analysis; C.M, L.B., A.T., N.S., H.H.F., C.M., M.R. and J.B. contributed to the
640 supervision of the work. All authors discussed the results and contributed to the final manuscript.

641 **CODE AVAILABILITY**

642 The STREAM model version 1.3, with a short user manual, is freely downloadable in Zenodo
643 (<https://zenodo.org/record/4744984>, doi: 10.5281/zenodo.4744984). The STREAM v1.3 model code
644 is distributed through M language files, but it could be run with different interpreters of M language,
645 like the GNU Octave (freely downloadable here <https://www.gnu.org/software/octave/download>).

646 **DATA AVAILABILITY**

647 All data and codes used in the study are freely available online. Air temperature data are available at
648 <https://psl.noaa.gov/data/gridded/data.cpc.globaltemp.html> (last access 25/11/202). In situ river
649 discharge data have been taken from the Global Runoff Data Center (GRDC,
650 https://www.bafg.de/GRDC/EN/Home/homepage_node.html (last access 25/11/202). Precipitation
651 and soil moisture data are available from <http://pmm.nasa.gov/data-access/downloads/trmm> and
652 <https://esa-soilmoisture-cci.org/>, respectively.

653 **COMPETING INTERESTS**

654 The authors declare that they have no conflict of interest.

655 **ACKNOWLEDGMENTS**

656 The authors wish to thank the Global Runoff Data Centre (GRDC) for providing most of the
657 streamflow data throughout Europe. The authors gratefully acknowledge support from ESA through
658 the STREAM Project (EO Science for Society element Permanent Open Call contract n°
659 4000126745/19/I-NB).

660

661 REFERENCE

- 662 Albergel, C., Rüdiger, C., Carrer, D., Calvet, J. C., Fritz, N., Naeimi, V., Bartalis, Z., and Hasenauer, S.: An evaluation
663 of ASCAT surface soil moisture products with in-situ observations in southwestern France, *Hydrol. Earth Syst. Sci.*,
664 13, 115–124, <https://doi.org/doi:10.5194/hess-13-115-2009>, 2009.
- 665 Alcamo, J., Döll, P., Henrichs, T., Kaspar, F., Lehner, B., Rösch, T., & Siebert, S.: Development and testing of the
666 WaterGAP 2 global model of water use and availability, *Hydrol. Sci. J.*, 48(3), 317–337,
667 <https://doi.org/10.1623/hysj.48.3.317.45290>, 2003.
- 668 Alexander, J. S., Wilson, R. C., and Green, W. R.: A brief history and summary of the effects of river engineering and
669 dams on the Mississippi River system and delta (p. 53), US Department of the Interior, US Geological Survey,
670 <https://doi.org/10.3133/cir1375>, 2012.
- 671 Allen, R.G., Pereira, L. S., Raes, D., and Smith, M.: Crop evapotranspiration — guidelines for computing crop water
672 requirements. FAO Irrigation & Drainage Paper 56. FAO, Rome, 1988.
- 673 Arabzadeh, A., and Behrangi, A.: Investigating Various Products of IMERG for Precipitation Retrieval Over Surfaces
674 With and Without Snow and Ice Cover, *Remote Sens.*, 13(14), 2726; <https://doi.org/10.3390/rs13142726>, 2021.
- 675 Balsamo, G., A. Beljaars, K. Scipal, P. Viterbo, B. vanden Hurk, M. Hirschi, and A. K. Betts: A revised hydrology for
676 the ECMWF model: Verification from field site to terrestrial water storage and impact in the integrated forecast
677 system, *J. Hydrometeorol.*, 10(3), 623–643, <https://doi.org/doi:10.1175/2008JHM1068.1>, 2009.
- 678 Barbarossa, V., Huijbregts, M. A., Beusen, A. H., Beck, H. E., King, H., and Schipper, A. M.: FLO1K, global maps of
679 mean, maximum and minimum annual streamflow at 1 km resolution from 1960 through 2015, *Scientific Data*,
680 5, 180052, <https://doi.org/10.1038/sdata.2018.52>, 2018.
- 681 Beck, H. E., van Dijk, A. I., de Roo, A., Dutra, E., Fink, G., Orth, R., and Schellekens, J.: Global evaluation of runoff
682 from ten state-of-the-art hydrological models, *Hydrol. Earth Syst. Sci.*, 21(6), 2881–2903. <https://doi.org/doi:10.5194/hess-21-2881-2017>, 2017.
- 684 Berghuijs, W. R., Woods, R. A., Hutton, C. J., and Sivapalan, M.: Dominant flood generating mechanisms across the
685 United States, *Geophys. Res. Lett.*, 43, 4382–4390, <https://doi.org/10.1002/2016GL068070>, 2016.
- 686 Berthet, L., Andréassian, V., Perrin, C., and Javelle, P.: How crucial is it to account for the antecedent moisture conditions
687 in flood forecasting? Comparison of event-based and continuous approaches on 178 catchments, *Hydrol. Earth Syst.*
688 *Sci.*, 13(6), 819–831, 2009.
- 689 Blöschl, G., Sivapalan, M., Wagener, T., Viglione, A., and Savenije, H. H. G. (Eds.): *Runoff predictions in ungauged*
690 *basins: A synthesis across processes, places and scales*, Cambridge: Cambridge University Press, 2013.
- 691 Bober, W. *Introduction to Numerical and Analytical Methods with MATLAB for Engineers and Scientists*; CRC Press,
692 Inc.: Boca Raton, FL, USA, <https://doi.org/10.1201/b16030>, 2013.
- 693 Botter, G., Porporato, A., Daly, E., Rodriguez-Iturbe, I., and Rinaldo, A.: Probabilistic characterization of base flows in
694 river basins: Roles of soil, vegetation, and geomorphology, *Water Resour. Res.*, 43, W06404,
695 <https://doi.org/doi:10.1029/2006WR005397>, 2007a.
- 696 Botter, G., Peratoner, F., Porporato, A., Rodriguez-Iturbe, I., and Rinaldo, A.: Signatures of large-scale soil moisture
697 dynamics on streamflow statistics across U.S. Climate regimes, *Water Resour. Res.*, 43, W11413,
698 <https://doi.org/doi:10.1029/2007WR006162>, 2007b.
- 699 Brocca, L., Melone, F., and Moramarco, T.: On the estimation of antecedent wetness conditions in rainfall-runoff
700 modelling, *Hydrol. Process.*, 22 (5), 629–642, doi:10.1002/hyp.6629. <https://doi.org/10.1002/hyp.6629>, 2008.
- 701 Brocca, L., Melone, F., Moramarco, T., and Morbidelli, R.: Antecedent wetness conditions based on ERS scatterometer
702 data, *J. Hydrol.*, 364(1–2), 73–87, <https://doi.org/10.1016/j.jhydrol.2008.10.007>, 2009.
- 703 Brocca, L., Melone, F., and Moramarco, T.: Distributed rainfall-runoff modelling for flood frequency estimation and
704 flood forecasting, *Hydrol. Process.*, 25(18), 2801–2813, <https://doi.org/10.1002/hyp.8042>, 2011.

705 Brocca, L., Ciabatta, L., Massari, C., Camici, S., and Tarpanelli, A.: Soil moisture for hydrological applications: open
706 questions and new opportunities, *Water*, 9(2), 140, <https://doi.org/10.3390/w9020140>, 2017.

707 Cai, X., Yang, Z. L., David, C. H., Niu, G. Y., and Rodell, M.: Hydrological evaluation of the Noah-MP land surface
708 model for the Mississippi River Basin, *J. Geophys. Res. Atmos.*, 119(1), 23-38,
709 <https://doi.org/10.1002/2013JD020792>, 2014.

710 Cislighi, A., Masseroni, D., Massari, C., Camici, S., and Brocca, L.: Combining a rainfall-runoff model and a
711 regionalization approach for flood and water resource assessment in the western Po Valley, Italy, *Hydrol. Sci. J.*,
712 65(3), 348-370, <https://doi.org/10.1080/02626667.2019.1690656>, 2020.

713 Crochemore, L., Isberg, K., Pimentel, R., Pineda, L., Hasan, A., and Arheimer, B.: Lessons learnt from checking the
714 quality of openly accessible river flow data worldwide, *Hydrol. Sci. J.*, 65(5), 699-711,
715 <https://doi.org/10.1080/02626667.2019.1659509>, 2020.

716 Crow, W. T., Bindlish, R., and Jackson, T. J.: The added value of spaceborne passive microwave soil moisture retrievals
717 for forecasting rainfall-runoff partitioning, *Geophys. Res. Lett.*, 32(18), <https://doi.org/10.1029/2005GL023543>,
718 2005.

719 Döll, P., F.Kaspar, and B.Lehner: A global hydrological model for deriving water availability indicators: Model tuning
720 and validation, *J. Hydrol.*, 270(1-2), 105-134, [https://doi.org/doi:10.1016/S0022-1694\(02\)00283-4](https://doi.org/doi:10.1016/S0022-1694(02)00283-4), 2003.

721 Dorigo, W., Wagner, W., Albergel, C., Albrecht, F., Balsamo, G., Brocca, L., Chung, D., Ertl, M., Forkel, M., Gruber, A.,
722 Haas, D., Hamer, P., Hirschi, M., Ikonen, J., de Jeu, R., Kidd, R., Lahoz, W., Liu, Y.Y., Miralles, D., Mistelbauer, T.,
723 Nicolai-Shaw, N., Parinussa, R., Pratola, C., Reimer, C., van der Schalie, R., Seneviratne, S.I., Smolander, T., and
724 Lecomte, P.: ESA CCI Soil Moisture for improved Earth system understanding: state-of-the art and future directions.,
725 *Remote Sens. Environ.*, 203, 185-215, <https://doi.org/10.1016/j.rse.2017.07.001>, 2017.

726 Dyer, J.: Snow depth and streamflow relationships in large North American watersheds, *J. Geophys. Res.*, 113, D18113,
727 <https://doi.org/10.1029/2008JD010031>, 2008.

728 Entekhabi, D., Njoku, E. G., O'Neill, P. E., Kellogg, K. H., Crow, W. T., Edelstein, W. N., ... and Van Zyl, J.: The soil
729 moisture active passive (SMAP) mission. *Proceedings of the Institute of Electrical and Electronics Engineers (IEEE)*,
730 98(5), 704-716. <https://doi.org/doi:10.1109/JPROC.2010.2043918>, 2010.

731 Famiglietti, J.S., and Wood, E. F.: Multiscale modeling of spatially variable water and energy balance processes, *Water*
732 *Resour. Res.*, 30, 3061-3078, <https://doi.org/10.1029/94WR01498>, 1994.

733 Famiglietti, J. S., and Rodell, M.: Water in the balance, *Science*, 340(6138), 1300-1301,
734 <https://doi.org/10.1126/science.1236460>, 2013.

735 Fan, Y. and Van den Dool, H. A: Global monthly land surface air temperature analysis for 1948-present, *J. Geophys.*
736 *Res. Atmos.*, 113, D01103, <https://doi.org/10.1029/2007JD008470>, 2008.

737 Fekete, B. M., Looser, U., Pietroniro, A., and Robarts, R. D.: Rationale for monitoring discharge on the ground, *J.*
738 *Hydrometeorol.*, 13, 1977-1986, <https://doi.org/10.1175/JHM-D-11-0126.1>, 2012.

739 Georgakakos KP, and Baumer OW.: Measurement and utilization of onsite soil moisture data, *J. Hydrol.*, 184: , 131-152,
740 [https://doi.org/10.1016/0022-1694\(95\)02971-0](https://doi.org/10.1016/0022-1694(95)02971-0), 1996.

741 Ghiggi, G., Humphrey, V., Seneviratne, S. I., and Gudmundsson, L.: GRUN: an observation-based global gridded runoff
742 dataset from 1902 to 2014, *Earth Syst. Sci. Data*, 11, 1655-1674 *Earth System Science Data*, 11(4), 1655-1674,
743 <https://doi.org/10.5194/essd-11-1655-2019>, 2019.

744 Ghotbi, S., Wang, D., Singh, A., Blöschl, G., and Sivapalan, M.: A New Framework for Exploring Process Controls of
745 Flow Duration Curves, *Water Resour. Res. Water Resources Research*, 56(1), <https://doi.org/e2019WR026083>, 2020.

746 Gochis, D. J., Barlage, M., Dugger, A., FitzGerald, K., Karsten, L., McAllister, M., et al. (2018). The WRF-Hydro
747 modeling system technical description, (Version 5.0). NCAR Technical Note. Retrieved from
748 <https://ral.ucar.edu/sites/default/files/public/WRFHydroV5TechnicalDescription.pdf>

749 Gudmundsson, L., Wagener, T., Tallaksen, L. M., and Engeland, K.: Evaluation of nine large-scale hydrological models
750 with respect to the seasonal runoff climatology in Europe, *Water Resour. Res.*, 48(11),
751 <https://doi.org/10.1029/2011WR010911>, 2012a.

752 Gudmundsson, L., Tallaksen, L. M., Stahl, K., Clark, D. B., Du-mont, E., Hagemann, S., Bertrand, N., Gerten, D., Heinke,
753 J., Hanasaki, N., Voss, F., and Koirala, S.: Comparing Large-Scale Hydrological Model Simulations to Observed
754 Runoff Percentiles in Europe, *J. Hydrometeorol.*, 13, 604–62, <https://doi.org/10.1175/JHM-D-11-083.1>, 2012b.

755 Gudmundsson, L., and Seneviratne, S. I.: Observation-based gridded runoff estimates for Europe (E-RUN version 1.1),
756 *Earth Syst. Sci. Data*, 8, 279–295, <https://doi.org/10.5194/essd-8-279-2016>, 8(2), 279-295 2016, 2016.

757 Gupta VK, Waymire E, and Wang CT.: A representation of an instantaneous unit hydrograph from geomorphology, *Water*
758 *Resour. Res.*, 16: 855–862, <https://doi.org/doi:10.1029/WR016i005p00855>, 1980.

759 Gupta, H. V., Kling, H., Yilmaz, K. K., and Martinez, G. F.: Decomposition of the mean squared error and NSE
760 performance criteria: Implications for improving hydrological modelling, *J. Hydrol.*, 377(1-2), 80-91,
761 <https://doi.org/10.1016/j.jhydrol.2009.08.003>, 2009.

762 Haddeland, I., Heinke, J., Voß, F., Eisner, S., Chen, C., Hagemann, S., and Ludwig, F.: Effects of climate model radiation,
763 humidity and wind estimates on hydrological simulations, *Hydrol. Earth Syst. Sci.*, 16(2), 305-318,
764 <https://doi.org/10.5194/hess-16-305-2012>, 2012.

765 Hanasaki, N., Kanae, S., Oki, T., Masuda, K., Motoya, K., Shirakawa, N., ... , and Tanaka, K. :An integrated model for
766 the assessment of global water resources–Part 1: Model description and input meteorological forcing, *Hydrol. Earth*
767 *Syst. Sci.*, 12(4), 1007-1025, <https://doi.org/10.5194/hess-12-1007-2008>, 2008.

768 Hastie, T., Tibshirani, R., and Friedman, J. H.: The Elements of Statistical Learning – Data Mining, Inference, and
769 Prediction, Second Edition, Springer Series in Statistics, Springer, New York, 2nd Edn., available at: [http://www-](http://www-stat.stanford.edu/~tibs/ElemStatLearn/)
770 [stat.stanford.edu/~tibs/ElemStatLearn/](http://www-stat.stanford.edu/~tibs/ElemStatLearn/) (last access: 5 July 2016)., 2009.

771 Hong, Y., Adler, R. F., Hossain, F., Curtis, S., and Huffman, G. J.: A first approach to global runoff simulation using
772 satellite rainfall estimation, *Water Resour. Res.*, 43(8), <https://doi.org/10.1029/2006WR005739>, 2007.

773 Horton, R. E.: Hydrological approach to quantitative morphology, *Geol. Soc. Am. Bull.*, 56, 275-370, 1945.

774 Houborg, R., Rodell, M., Li, B., Reichle, R., and Zaitchik, B. F.: Drought indicators based on model-assimilated Gravity
775 Recovery and Climate Experiment (GRACE) terrestrial water storage observations, *Water Resour. Res.*, 48(7),
776 <https://doi.org/10.1029/2011WR011291>, 2012.

777 Hu GR., and Li XY.: Subsurface Flow. In: Li X., Vereecken H. (eds) Observation and Measurement. Ecohydrology.
778 Springer, Berlin, Heidelberg. https://doi.org/10.1007/978-3-662-47871-4_9-1, 2018.

779 Huffman, G. J., Adler, R. F., Bolvin, D. T., Gu, G. J., Nelkin, E. J., Bowman, K. P., Hong, Y., Stocker, E. F. and Wolff,
780 D. B.: The TRMM Multisatellite Precipitation Analysis (TMPA): Quasi-Global, Multiyear, Combined-Sensor
781 Precipitation Estimates at Fine Scales, *J. Hydrometeorol.*, 8 (1): 38–55. <https://doi.org/doi:10.1175/jhm560.1>, 2007.

782 Huffman, G. J., Stocker, E. F., Bolvin, D. T., Nelkin, E. J., and Adler, R. F.: TRMM Version 7 3B42 and 3B43 Data Sets.
783 NASA/GSFC, Greenbelt, MD, 2014.

784 Huffman, G. J., Bolvin, D. T., Braithwaite D., Hsu K., Joyce R. , Kidd C., Nelkin Eric J., Sorooshian S., Tan J., and Xie
785 P.: NASA Global Precipitation Measurement (GPM) Integrated Multi-satellitE Retrievals for GPM (IMERG),.
786 https://docsserver.gesdisc.eosdis.nasa.gov/public/project/GPM/IMERG_ATBD_V06.pdf, 2019.

787 Kauffeldt, A., Wetterhall, F., Pappenberger, F., Salamon, P., & Thielen, J.: Technical review of large-scale hydrological
788 models for implementation in operational flood forecasting schemes on continental level, *Environ. Model. Softw.*, 75,
789 68-76, <https://doi.org/10.1016/j.envsoft.2015.09.009>, 2016.

790 Kim, H., Watanabe, S., Chang, E. C., Yoshimura, K., Hirabayashi, J., Famiglietti, J., and Oki, T.: Global Soil Wetness
791 Project Phase 3 Atmospheric Boundary Conditions (Experiment 1) [Data set], Data Integration and Analysis System
792 (DIAS), <https://doi.org/10.20783/DIAS.501>, 2017.

793 Kirchner, J. W.: Getting the right answers for the right reasons: Linking measurements, analyses, and models to advance
794 the science of hydrology, *Water Resour. Res.*, 42(3), <https://doi.org/10.1029/2005WR004362>, 2006.

795 Klees, R., Revtova, E. A., Gunter, B.C. , Ditmar, P., Oudman, E., Winsemius H. C., and Savenije H.H.G.: The design of
796 an optimal filter for monthly GRACE gravity models, *Geoph. J. Intern.*, 175 (2): 417–432,
797 <https://doi.org/10.1111/j.1365-246X.2008.03922.x>, 2008

798 Kling, H., Fuchs, M., and Paulin, M.: Runoff conditions in the upper Danube basin under an ensemble of climate change
799 scenarios, *J. Hydrol.*, 424, 264-277, <https://doi.org/doi:10.1016/j.jhydrol.2012.01.011>, 2012.

800 Landerer, F. W., and Swenson, S. C.: Accuracy of scaled GRACE terrestrial water storage estimates, *Water Resour. Res.*,
801 48(4), <https://doi.org/10.1029/2011WR011453>, 2012.

802 Lehner, B., C. Reidy Liermann, C. Revenga, C. Vörösmarty, B. Fekete, P. Crouzet, P. Döll, M. Endejan, K. Frenken, J.
803 Magome, C. Nilsson, J.C. Robertson, R. Rodel, N. Sindorf, and D. Wisser.: High-resolution mapping of the world's
804 reservoirs and dams for sustainable river-flow management, *Front. Ecol. Environ.*, 9 (9),: 494-502,
805 <https://doi.org/10.1890/100125>, 2011.

806 Lindström, G., Pers, C., Rosberg, J., Strömquist, J., & Arheimer, B.: Development and testing of the HYPE (Hydrological
807 Predictions for the Environment) water quality model for different spatial scales, *Hydrol. Res.*, 41(3-4), 295-319,
808 <https://doi.org/10.2166/nh.2010.007>, 2010.

809 Long, D., Longuevergne, L., and Scanlon, B. R.: Uncertainty in evapotranspiration from land surface modeling, remote
810 sensing, and GRACE satellites, *Water Resour. Res.*, 50(2), 1131-1151, <https://doi.org/10.1002/2013WR014581>,
811 2014.

812 Lorenz, C., H. Kunstmann, H., B. Devaraju, B., Tourian, M. J., N. Sneeuw, N., and J. Riegger, J.: Large-Scale Runoff
813 from Landmasses: A Global Assessment of the Closure of the Hydrological and Atmospheric Water Balances., *J.*
814 *Hydrometeor.*, 15, 2111–2139, <https://doi.org/doi:10.1175/JHM-D-13-0157.1>, 2014.

815 Luthcke, S.B., Sabaka, T.J., Loomis, B.D., Arendt, A.A., McCarthy, J.J., and Camp, J.: Antarctica, Greenland and Gulf
816 of Alaska land-ice evolution from an iterated GRACE global mascon solution, *J. Glaciol.*, Vol. 59, No. 216, 613-631,
817 2013 <https://doi.org/doi:10.3189/2013JoG12J147>, 2013.

818 Massari, C., Brocca, L., Barbetta, S., Papathanasiou, C., Mimikou, M., and Moramarco, T.: Using globally available soil
819 moisture indicators for flood modelling in Mediterranean catchments, *Hydrol. Earth Syst. Sci.*, 18(2), 839,
820 <https://doi.org/10.5194/hess-18-839-2014>, 2014.

821 Massari, C., Brocca, L., Tarpanelli, A., Hong, Y., Crow, W., Ciabatta, L., Camici, S., Barbetta, S., and Moramarco, T.:
822 Global surface runoff estimation in near real time by using SMAP and GPM, poster at SMAP conference, 2016.

823 Maxwell, R. M., Condon, L. E., and Kollet, S. J.: A high-resolution simulation of groundwater and surface water over
824 most of the continental US with the integrated hydrologic model ParFlow v3, *Geosci. Model Dev.*, 8, 923–937,
825 <https://doi.org/10.5194/gmd-8-923-2015>, 2015.

826 Merz, R., and and Blöschl, G.: A regional analysis of event runoff coefficients with respect to climate and catchment
827 characteristics in Austria, *Water Resour. Res.*, 45(1), <https://doi.org/10.1029/2008WR007163>, 2009.

828 Mueller Schmied, H., Adam, L., Eisner, S., Fink, G., Flörke, M., Kim, H., ... and Song, Q.: Variations of global and
829 continental water balance components as impacted by climate forcing uncertainty and human water use, *Hydrol. Earth*
830 *Syst. Sci.*, 20(7), 2877-2898, <https://doi.org/10.5194/hess-20-2877-2016>, 2016.

831 Muneeppeerakul, R., Azaele, S., Botter, G., Rinaldo, A., and Rodriguez-Iturbe, I.: Daily streamflow analysis based on a
832 two-scaled gamma pulse model, *Water Resour. Res.*, 46(11), <https://doi.org/10.1029/2010WR009286>, 2010.

833 Nash, J. E.: The form of the instantaneous unit hydrograph, *IASH publication no. 45*, 3–4, 114–121, 1957.

834 Natural Resources Conservation Service (NRCS): Urban hydrology for small watersheds, Tech. Release 55, 2nd ed., U.S.
835 Dep. of Agric., Washington, D. C. (available at [ftp://ftp.wcc.nrcs.usda.gov/downloads/](ftp://ftp.wcc.nrcs.usda.gov/downloads/hydrology_hydraulics/tr55/tr55.pdf)
836 [hydrology_hydraulics/tr55/tr55.pdf](ftp://ftp.wcc.nrcs.usda.gov/downloads/hydrology_hydraulics/tr55/tr55.pdf)), 1986.

837 Oleson, K., Lawrence, D. M., Bonan, G. B., Drewniak, B., Huang, M., Koven, C. D., ... Yang, Z. -L.: Technical
838 description of version 4.5 of the Community Land Model (CLM) (No. NCAR/TN-503+STR).
839 <http://dx.doi.org/10.5065/D6RR1W7M>, 2013.

840 Orth, R., and Seneviratne, S. I.: Introduction of a simple-model-based land surface dataset for Europe, *Environ. Res. Lett.*,
841 10(4), 044012, <https://doi.org/10.1088/1748-9326/10/4/044012>, 2015.

842 Pellet, V., Aires, F., Munier, S., Fernández Prieto, D., Jordá, G., Dorigo, W. A., ... and Brocca, L.: Integrating multiple
843 satellite observations into a coherent dataset to monitor the full water cycle—application to the Mediterranean region.,
844 *Hydrol. Earth Syst. Sci.*, 23(1), 465-491, <https://doi.org/10.5194/hess-23-465-2019>, 2019.

845 Prudhomme, C., Giuntoli, I., Robinson, E. L., Clark, D. B., Arnell, N. W., Dankers, R., ... and Hagemann, S.: Hydrological
846 droughts in the 21st century, hotspots and uncertainties from a global multimodel ensemble experiment, *Proceedings*
847 *of the National Academy of Sciences*, 111(9), 3262-3267, 2014.

848 Rakovec, O., Kumar, R., Attinger, S., and Samaniego, L.: Improving the realism of hydrologic model functioning through
849 multivariate parameter estimation, *Water Resour. Res.*, 52(10), 7779-7792, <https://doi.org/10.1002/2016WR019430>,
850 2016.

851 Richards, L.A.: Capillary conduction of liquids through porous mediums, *Physics*. 1 (5): 318-333.,
852 Bibcode:1931Physi.1.318R., <https://doi.org/doi:10.1063/1.1745010>, 1931.

853 Riegger, J., and Tourian, M. J.: Characterization of runoff-storage relationships by satellite gravimetry and remote
854 sensing, *Water Resour. Res.*, 50, 3444-3466, <https://doi.org/doi:10.1002/2013WR013847>, 2014.

855 Rodell, M., Beaudoin, H. K., L'Ecuyer, T. S., Olson, W. S., Famiglietti, J. S., Houser, P. R., Adler, R., Bosilovich, M.
856 G., Clayson, C. A., Chambers, D., Clark, E., Fetzer, E. J., Gao, X., Gu, G., Hilburn, K., Huffman, G. J., Lettenmaier,
857 D. P., Liu, W. T., Robertson, F. R., Schlosser, C. A., Sheffield, J. and Wood, E. F.: The observed state of the water
858 cycle in the early 15twenty-first century, *J. Clim.*, 28(21), 8289-8318, [https://doi.org/doi:10.1175/JCLI-D-14-](https://doi.org/doi:10.1175/JCLI-D-14-00555.1)
859 [00555.1](https://doi.org/doi:10.1175/JCLI-D-14-00555.1), 2015.

860 Schellekens, J., Dutra, E., Martínez-de la Torre, A., Balsamo, G., van Dijk, A., Sperna Weiland, F., Minvielle, M., Cal-
861 vet, J.-C., Decharme, B., Eisner, S., Fink, G., Flörke, M., Peßenteiner, S., van Beek, R., Polcher, J., Beck, H., Orth, R.,
862 Calton, B., Burke, S., Dorigo, W., and Weedon, G. P.: A global water resources ensemble of hydrological models: the
863 earth2Observe Tier-1 dataset, *Earth Syst. Sci. Data*, 9, 389-413, <https://doi.org/10.5194/essd-9-389-2017>, 2017.

864 Schwanghart, W., and Kuhn, N. J.: TopoToolbox: A set of Matlab functions for topographic analysis., *Environ. Model.*
865 *Softw. Environmental Modelling & Software*, 25(6), 770-781, 2010.

866 Seneviratne, S. I., Corti, T., Davin, E. L., Hirschi, M., Jaeger, E. B., Lehner, I., ... and Teuling, A. J.: Investigating soil
867 moisture-climate interactions in a changing climate: A review, *Earth-Sci. Rev.*, 99(3-4), 125-161,
868 <https://doi.org/10.1016/j.earscirev.2010.02.004>, 2010.

869 Sneeuw, N., Lorenz, C., Devaraju, B., Tourian, M. J., Riegger, J., Kunstmann, H., and Bárdossy, A.: Estimating runoff
870 using hydro-geodetic approaches, *Surv. Geophys.*, 35(6), 1333-1359, <https://doi.org/10.1007/s10712-014-9300-4>,
871 2014.

872 Solomatine, D. P., and Ostfeld, A.: Data-driven modelling: some past experiences and new approaches, *J. Hydroinform.*,
873 10(1), 3-22, <https://doi.org/10.2166/hydro.2008.015>, 2008.

874 Sood, A., and Smakhtin, V.: Global hydrological models: a review, *Hydrol. Sci. J.*, 60(4), 549-565,
875 <https://doi.org/10.1080/02626667.2014.950580>, 2015.

876 Strahler, A. N.: Hypsometric (area-altitude) analysis of erosional topography, *Geol. Soc. Am. Bull. Geological Society of*
877 *America Bulletin*, 63(11), 1117-1142, [https://doi.org/10.1130/0016-7606\(1952\)63\[1117:HAAOET\]2.0.CO;2](https://doi.org/10.1130/0016-7606(1952)63[1117:HAAOET]2.0.CO;2), 1952.

878 Tapley, B.D., Watkins, M.M., Flechtner, F. et al.: Contributions of GRACE to understanding climate change, *Nat. Clim.*
879 *Chang.*, 9, 358-369, <https://doi.org/doi:10.1038/s41558-019-0456-2>, 2019.

880 Thiémié, V., Rojas, R., Zambrano-Bigiarini, M., and De Roo, A.: Hydrological evaluation of satellite rainfall estimates
881 over the Volta and Baro-Akobo Basin, *J. Hydrol.*, 499, 324-338, <https://doi.org/10.1016/j.jhydrol.2013.07.012>, 2013.

882 Tourian, M. J., Reager, J. T., and Sneeuw, N.: The total drainable water storage of the Amazon river basin: A first estimate
883 using GRACE, *Water Resour. Res.*, 54., <https://doi.org/10.1029/2017WR021674>, 2018.

884 Trambly, Y., Bouvier, C., Martin, C., Didon-Lescot, J. F., Todorovik, D., and Domergue, J. M.: Assessment of initial
885 soil moisture conditions for event-based rainfall-runoff modelling, *J. Hydrol.*, 387(3-4), 176-187,
886 <https://doi.org/10.1016/j.jhydrol.2010.04.006>, 2010.

887 Troutman, B. M., and Karlinger, M.B.: Unit hydrograph approximation assuming linear flow through topologically
888 random channel networks, *Water Resour. Res.*, 21., 743 - 754, <https://doi.org/doi:10.1029/WR021i005p00743>, 1985.

889 Van Beek, L. P. H., and Bierkens, M. F. P.: The global hydrological model PCR-GLOBWB: conceptualization,
890 parameterization and verification. Utrecht University, Utrecht, The Netherlands, 1, 25-26, 2009.

891 Vörösmarty C. J., and Coauthors: Global water data: A newly endangered species, *Eos, Trans. Amer. Geophys. Union*,
892 82, 54, <https://doi.org/10.1029/01EO00031>, 2002.

893 Vose, R.S., Applequist, S., Durre, I., Menne, M.J., Williams, C.N., Fenimore, C., Gleason, K., and Arndt, D.: Improved
894 Historical Temperature and Precipitation on Time Series For U.S. Climate Divisions., *J. Meteorol. and Climat.*,
895 53(May), 1232–1251., <https://doi.org/10.1175/JAMC-D-13-0248.1>DOI: 10.1175/JAMC-D-13-0248.1, 2014.

896 Wagner, W., Lemoine, G., and Rott, H.: A method for estimating soil moisture from ERS scatterometer and soil data.,
897 *Remote Sens. Environ. Remote Sensing of Environment*, 70, 191–207, [https://doi.org/doi:10.1016/S0034-](https://doi.org/doi:10.1016/S0034-4257(99)00036-X)
898 [4257\(99\)00036-X](https://doi.org/doi:10.1016/S0034-4257(99)00036-X), 1999.

899 Wagner, W., Blöschl, G., Pampaloni, P., Calvet, J. C., Bizzarri, B., Wigneron, J. P., and Kerr, Y.: Operational readiness
900 of microwave remote sensing of soil moisture for hydrologic applications, *Hydrol. Res.*, 38(1), 1-20,
901 <https://doi.org/10.2166/nh.2007.029>, 2007.

902 Wang, Y. H., Broxton, P., Fang, Y., Behrangi, A., Barlage, M., Zeng, X., and Niu, G. Y.: A wet-bulb temperature-based
903 rain-snow partitioning scheme improves snowpack prediction over the drier western United States, *Geophys. Res.*
904 *Lett.*, 46(23), 13825-13835, <https://doi.org/10.1029/2019GL085722>, 2019.

905 Wisser, D., Fekete, B. M., Vörösmarty, C. J., and Schumann, A. H.: Reconstructing 20th century global hydrography: a
906 contribution to the Global Terrestrial Network- Hydrology (GTN-H), *Hydrol. Earth Syst. Sci.*, 14, 1–24,
907 <https://doi.org/doi:10.5194/hess-14-1-2010>, 2010.

908 Yokoo, Y., and Sivapalan, M.: Towards reconstruction of the flow duration curve: Development of a conceptual
909 framework with a physical basis, *Hydrol. Earth Syst. Sci.*, 15(9), 2805–2819, [https://doi.org/10.5194/hess-15-2805-](https://doi.org/10.5194/hess-15-2805-2011)
910 2011, 2011.

911 Zhang, Y., Pan, M., Sheffield, J., Siemann, A. L., Fisher, C. K., Liang, M., ... and Zhou, T.: A Climate Data Record
912 (CDR) for the global terrestrial water budget: 1984–2010, *Hydrol. Earth Syst. Sci.*, 22, 241–263,
913 [https://doi.org/10.5194/hess-22-241-2018\(Online\)](https://doi.org/10.5194/hess-22-241-2018(Online)), 22(PNNL-SA-129750), 2018.

915 Table 1. Location of gauging stations over the Mississippi basins and upstream contributing area.
 916 Bold text is used to indicate stations where the STREAM v1.3 model has been calibrated.

#	River	Station name	Latitude (°)	Longitude (°)	Upstream area (km ²)	Mean annual river discharge (m ³ /s)	Presence of dam
1	Missouri	Bismarck, ND	-100.82	46.81	481'232	633	Garrison dam
2	Missouri	Omaha, NE	-95.92	41.26	814'371	914	Gavins Point Dam
3	Missouri	Kansas City, MO	-94.59	39.11	1'229'427	1499	---
4	Missouri	Hermann, MO	-91.44	38.71	1'330'000	2326	---
5	Kansas	Wamego, KS	-96.30	39.20	143'054	141	Kanopolis
6	Mississippi	Keokuk, IA	-91.37	40.39	282'559	1948	---
7	Rock	Near Joslin, IL	-90.18	41.56	23'835	199	---
8	Mississippi	Chester, IL	-89.84	37.90	1'776'221	6018	---
9	Arkansas	Murray Dam Near Little Rock, AR	-92.36	34.79	408'068	1249	---
10	Mississippi	Vicksburg, MS	-90.91	32.32	2'866'590	17487	---
11	Ohio	Metropolis, ILL.	-88.74	37.15	496'134	7931	---

917
 918

919 Table 2. Performance scores obtained over the Mississippi river sections during the calibration and
920 validation periods.

#	CALIBRATION PERIOD			VALIDATION PERIOD		
SCORE	KGE (-)	R (-)	RRMSE (%)	KGE (-)	R (-)	RRMSE (%)
CALIBRATED SECTIONS						
10	0.78	0.78	30	0.74	0.80	38
9	0.62	0.75	71	0.67	0.85	77
6	0.83	0.84	39	0.73	0.84	46
4	0.77	0.78	46	0.72	0.75	50
11	0.82	0.82	44	0.70	0.86	51
SECTIONS NOT USED FOR CALIBRATION						
1	-3.26	0.08	137	0.20	0.44	96
2	-0.57	0.48	118	0.40	0.53	89
3	0.16	0.71	83	0.39	0.70	72
5	-1.49	0.24	368	-1.26	0.31	358
7	0.53	0.68	71	0.20	0.70	81
8	0.80	0.84	36	0.77	0.84	39

921

922

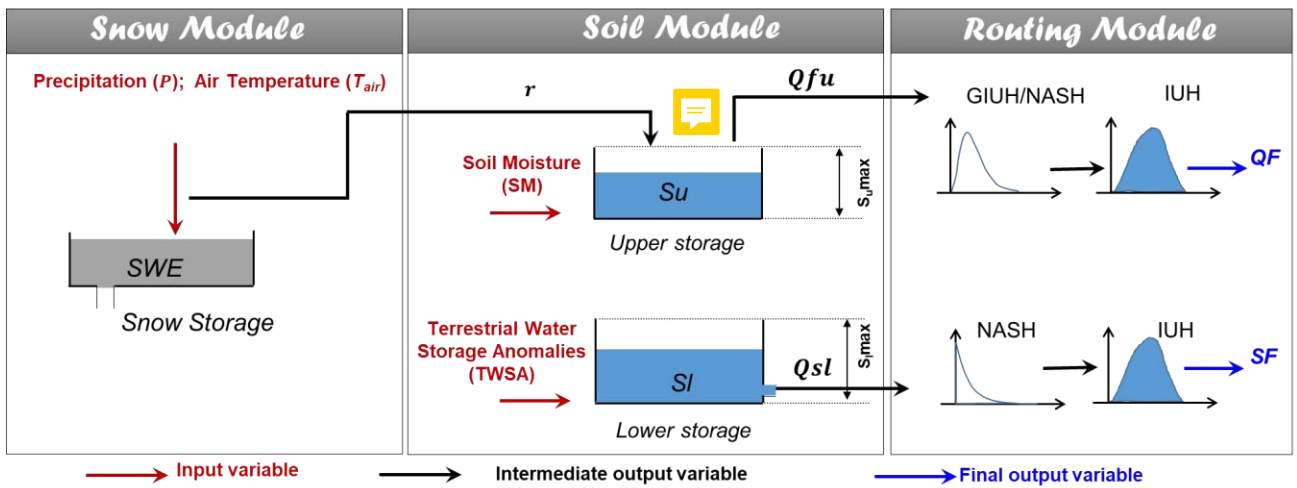
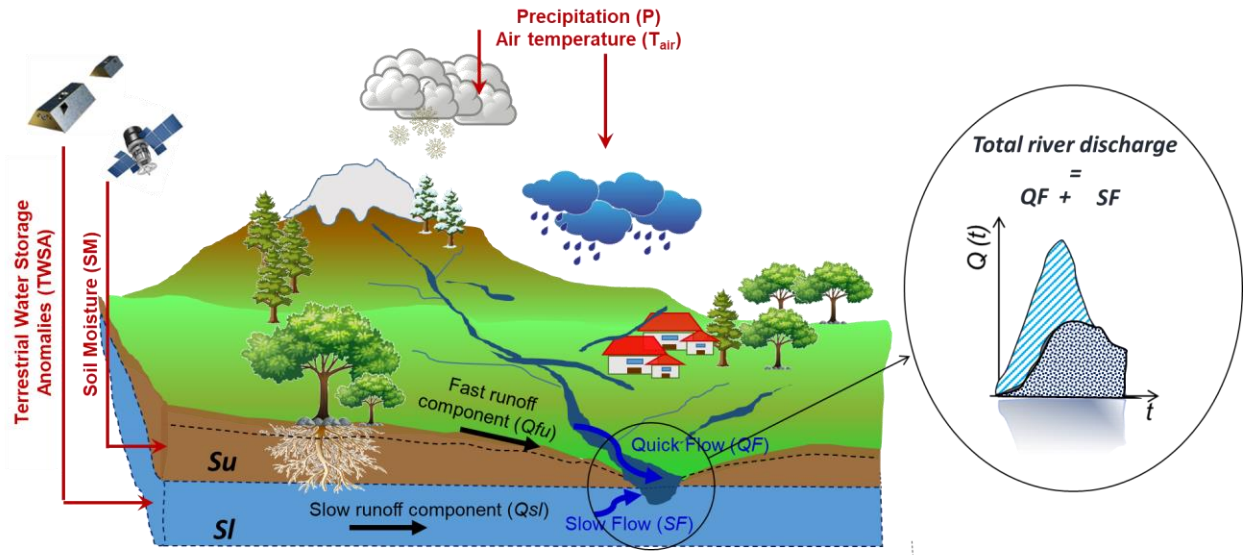
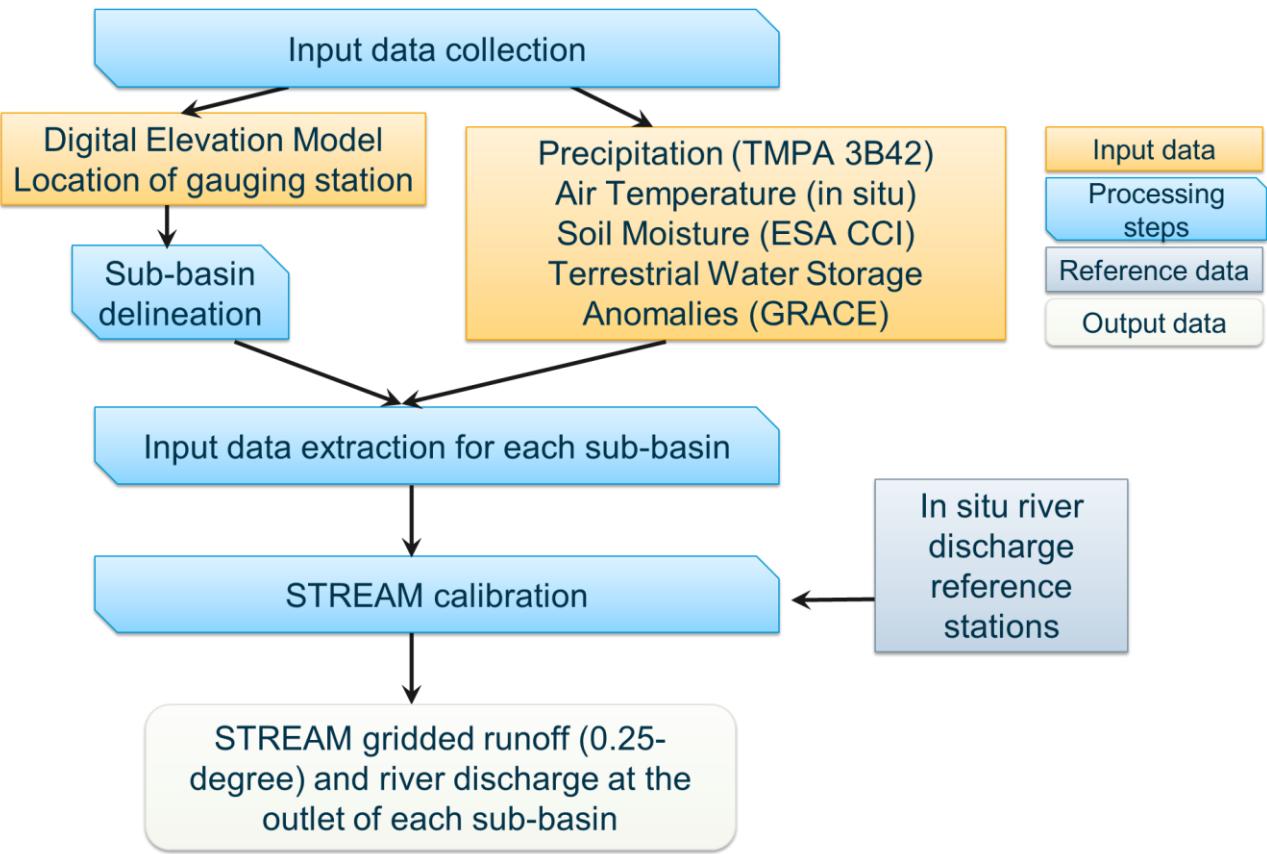


Figure 1. Configuration of the STREAM v1.3 model adopted for total runoff estimation. The model includes three modules, the snow module allowing to separate snowfall from precipitation, the soil module that simulates the slow and quick runoff components (Q_{su} and Q_{fu} , respectively) and the routing module for flood simulation. Red arrows indicate input variables; black arrows indicate intermediate output variables; blue arrows indicate final output variables. The components Q_{fu} and Q_{su} are computed by using satellite P , soil moisture and TWSA data as input to the soil module. Please refer to text for symbols.

932



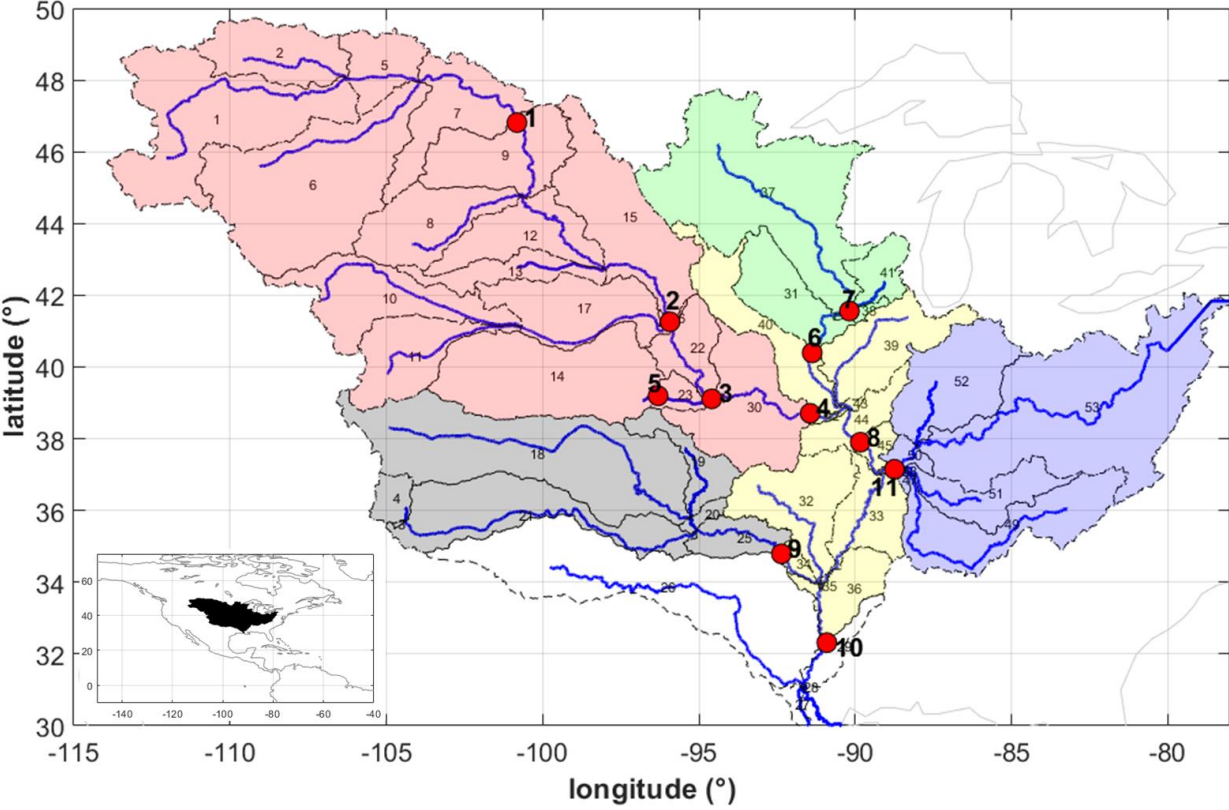
933

934

935 Figure 2. Processing steps of the STREAM v1.3 model.

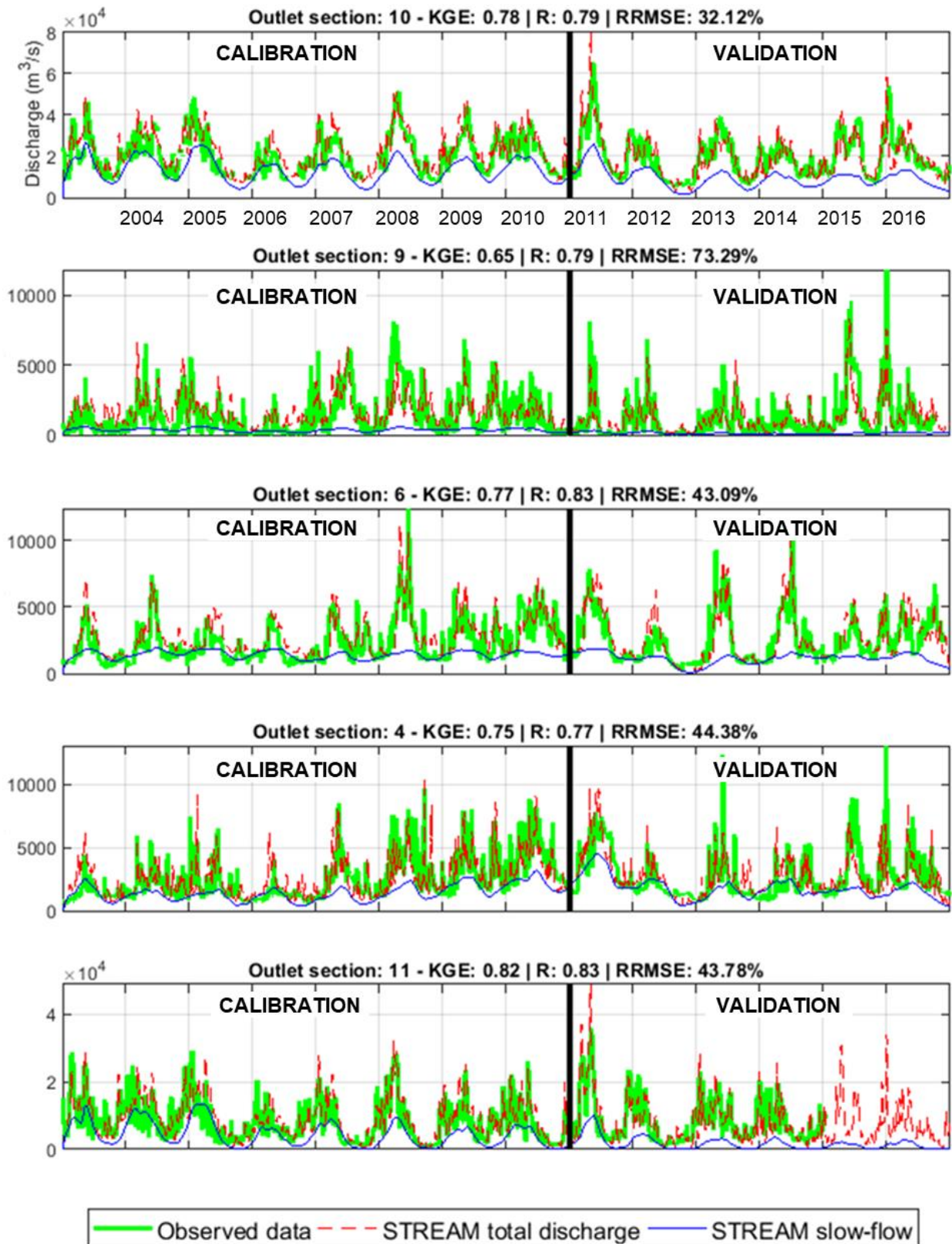
936

937



938

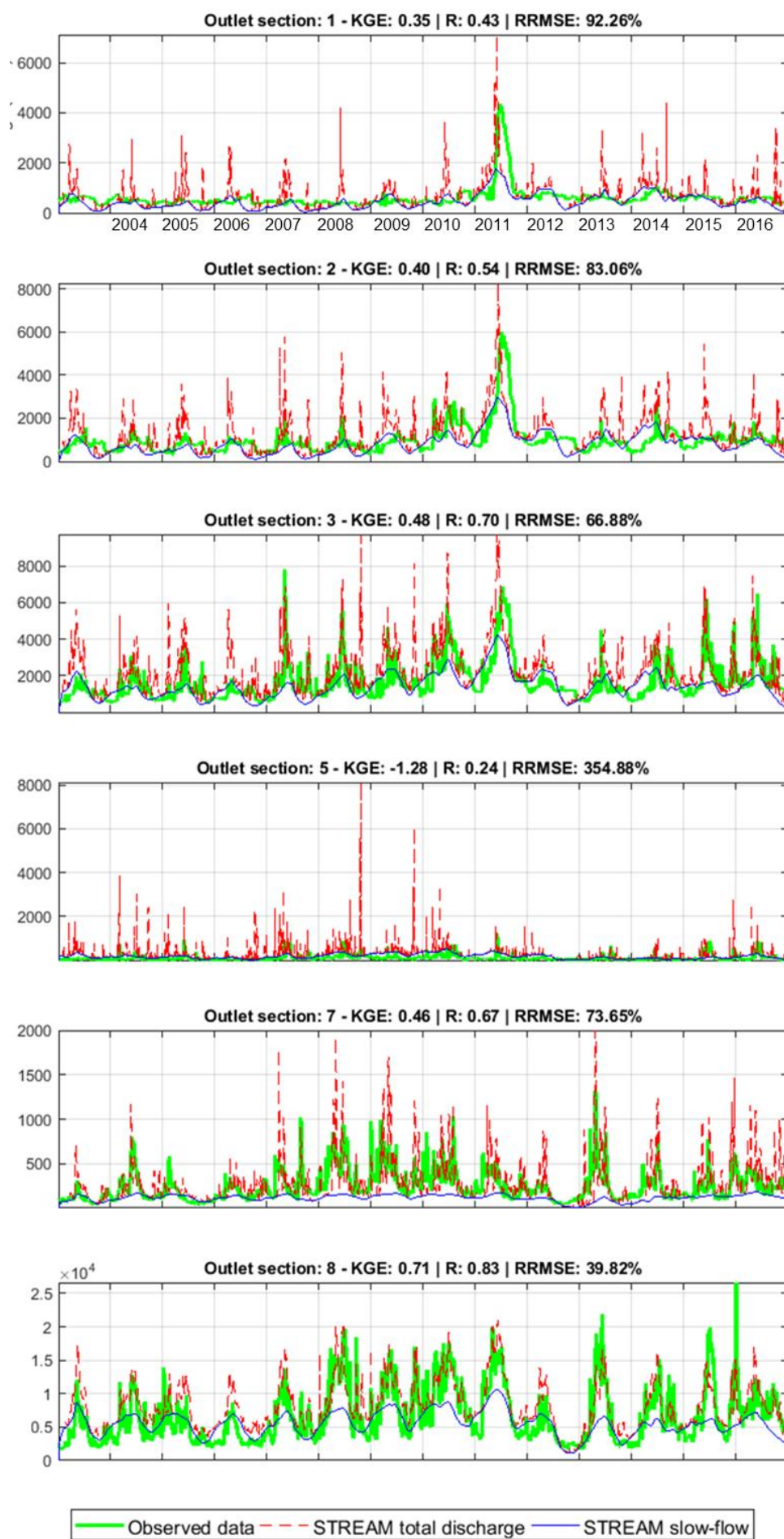
939 Figure 3. Mississippi sub-basin delineation. Red dots indicate the location of the discharge gauging
940 stations; different colours identify different inner sections (and the related contributing sub-basins)
941 used for the model calibration.
942



943

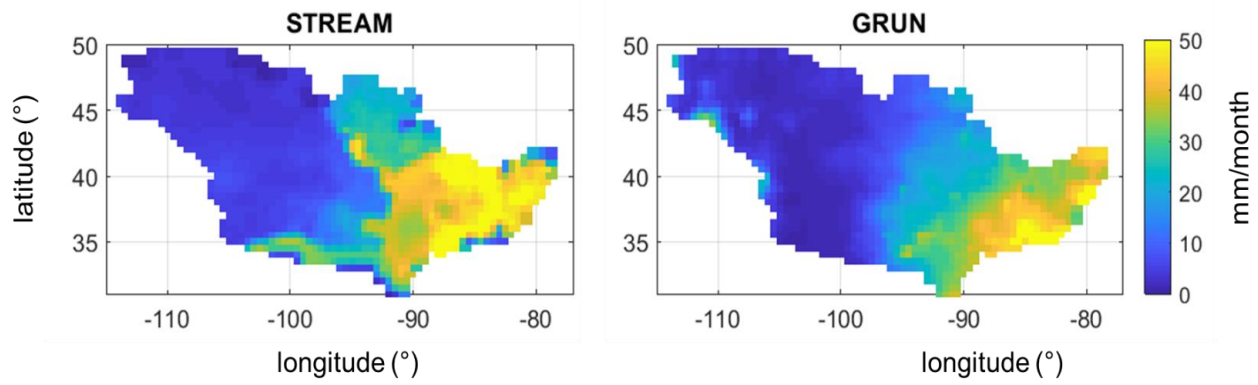
944 Figure 4. Comparison between observed and simulated river discharge time series over the five
 945 calibrated sections over Mississippi river basin. Performance scores at the top of each plot refer to
 946 the entire study period (2003–2016).

947



940
951
952
953
954

Figure 5. Comparison between observed and simulated river discharge time series over the gauged sections not used in the calibration phase. Performance scores at the top of each plot refer to the entire study period (2003–2016).



955

956 Figure 6. Mississippi river basin: mean monthly runoff for the period 2003–2014 obtained by
 957 STREAM v1.3 and GRUN models.

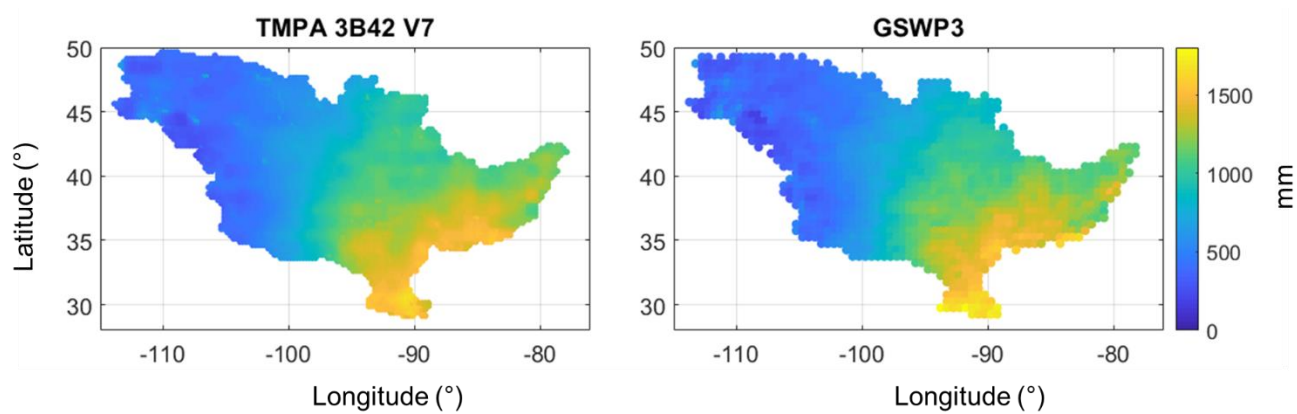
958

960 Table 1A. Description of STREAM v1.3 parameters, belonging module, variability range and unit.

Parameter	Description	Module	Range Variability	Unit
Cm	degree-day coefficient	Snow	0.1/24-3	[-]
α	exponent of infiltration	Soil	1-30	[-]
T	characteristic time length	Soil	0.01-80	[days]
β	coefficient relationship slow runoff component and TWSA	Soil	0.1-20	[mm h-1]
m	exponent in the relationship between slow runoff component and TWSA	Soil	1-15	[-]
γ	parameter of GIUH	Routing	0.5-5.5	[-]
C	Celerity	Routing	1-60	[km h-1]
D	Diffusivity	Routing	1-30	[km2 h-1]

961

962



963

964 Figure S1. Mean annual precipitation data over the period 2003-2014 obtained by TMPA 3B42 V7
 965 and GSWP3 datasets over the Mississippi river basin.

966